Preprint title: Circadian protein regulation in the green lineage II. The clock gene circuit controls a phospho-dawn in *Arabidopsis thaliana*.

Title: The circadian clock gene circuit controls protein and phosphoprotein rhythms in *Arabidopsis thaliana*.

Running title: Clock gene regulation of the Arabidopsis (phospho)proteome

Authors:
Johanna Krahmer[1,2,5], Matthew Hindle[3], Laura K Perby[4], Tom H Nielsen[4], Gerben VanOoijen[2], Karen J Halliday[2], Thierry Le Bihan[1], Andrew J Millar[1]

Adresses:
[1]SynthSys and School of Biological Sciences, CH Waddington Building, Max Born Crescent, Kings Buildings, University of Edinburgh, Edinburgh, EH9 3BF, United Kingdom
[2]Institute for Molecular Plant Science, School of Biological Sciences, Daniel Rutherford Building, Building, Max Born Crescent, Kings Buildings, University of Edinburgh, Edinburgh, EH9 3BF, United Kingdom
[3]The Roslin Institute and Royal (Dick) School of Veterinary Studies, Easter Bush, Edinburgh, EH25 9RG, United Kingdom
[4]Department of Plant and Environmental Sciences, University of Copenhagen, Section for Molecular Plant Biology, Thorvaldsensvej 40, 1871 Frb. C, Denmark
[5]Present address: Center for Integrative Genomics, Faculty of Biology and Medicine, University of Lausanne, 1015 Lausanne, Switzerland

For all correspondence: Andrew J Millar, phone: +44 (0)131 651 3325, fax: +44 (0)131 651 9068, email: Andrew.Millar@ed.ac.uk

ORCID:
Johanna Krahmer: 0000-0001-7728-5110
Matthew Hindle: 0000-0002-6870-4069
Andrew Millar: 0000-0003-1756-3654

Abbreviations:

TTFL	Transcriptional translational feedback loop
NTO	non-transcriptional oscillator
F2KP	fructose-6-phosphate-2-kinase / phosphatase
CCA1	Circadian clock associated 1
CCA1-Ox	CCA1 overexpressor
CK	casein kinase
SNF-1	sucrose non-fermenting
SnRK	SNF-1 related kinase
TOC1	timing of CAB expression 1
TOC1-Ox	TOC1 overexpressor
PRX	peroxiredoxin
PCA	principal component analysis
Col-0	Columbia 0
ZT	Zeitgeber time
h	hour

WT	wildtype
GO	gene ontology
SEM	standard error of the mean
BH	Benjamini - Hochberg

Abstract

The 24-hour rhythmicity in the levels of many eukaryotic mRNAs contrasts with the long half-lives of most detected proteins. Such stable molecular species are not expected to reflect the RNA rhythms, emphasizing the need to test the circadian regulation of protein abundance and modification. Here we present circadian proteomic and comparable phosphoproteomic time-series from *Arabidopsis thaliana* plants, estimating that 0.4% of quantified proteins and a much larger proportion of quantified phospho-sites were rhythmic under constant light conditions. Approximately half of the quantified phospho-sites were most phosphorylated at subjective dawn, when SnRK1 protein kinase was a candidate regulator. A *CCA1*-over-expressing line that disables the plant clock gene circuit lacked most or all circadian protein phosphorylation, indicating that the phospho-dawn is regulated by the canonical clock mechanism. The few phospho-sites that fluctuated despite *CCA1*-over-expression still tended to peak in abundance close to subjective dawn, indicating that their temporal regulation was less dependent on the clock gene circuit. To test the potential functional relevance of our datasets, we conduct phosphomimetic experiments using the bifunctional enzyme fructose-6-phosphate-2-kinase / phosphatase (F2KP), as an example. The clock gene circuit controls diverse protein targets in metabolism and physiology *via* phosphorylation, including where the bulk abundance of the cognate proteins is arrhythmic.

Introduction

Most circadian observations in *Arabidopsis* can be explained by a genetic repressilator which is composed of a network of mostly negatively interacting transcription factors (Pokhilko *et al*, 2012; Fogelmark & Troein, 2014). In addition to transcriptional interactions, this transcriptional-translational feedback loop (TTFL) system requires post-translational modification of transcription factor proteins (van Ooijen & Millar, 2012). Phosphorylation of CCA1 by casein kinase (CK) 2 for example is necessary for the circadian clock function (Daniel *et al*, 2004).

Protein phosphorylation is involved in the circadian clock mechanism not only in plants but also in fungi, animals and cyanobacteria (Nishiwaki *et al*, 2004; van Ooijen & Millar, 2012). While the transcription factors of TTFLs in animals, fungi and plants are not evolutionarily conserved (van Ooijen & Millar, 2012), many kinases that play a role in circadian timekeeping across eukaryotes, are similar. For instance CK2 is also important for circadian timing in mammals (Maier *et al*, 2009) and fungi (Yang *et al*, 2003). Protein phosphorylation is also involved in the output of the circadian clock (Kusakina & Dodd, 2012). However, only one study has so far addressed the question of how pervasive circadian protein phosphorylation is (Choudhary *et al*, 2015).

In addition to TTFLs, circadian oscillations can be driven by mechanisms that are independent of rhythmic transcription, non-transcriptional oscillators (NTOs). The cyanobacterial circadian clock is based on rhythmic autophosphorylation of the KaiC protein together with the KaiA and KaiB protein

and this mechanism does not even require a living cell to create oscillations (Nakajima *et al*, 2005). Evidence for NTOs also exists in eukaryotes. O'Neill *et al*, 2011 found that in *Ostreococcus tauri* cells, which do not transcribe in extended darkness, the protein peroxiredoxin (PRX) is rhythmically over-oxidized during 3 days of constant darkness. The same overoxidation rhythm was found in red blood cells which are enucleated and therefore do not possess a TTFL (O'Neill & Reddy, 2011). Rhythmic PRX over-oxidation was also found in transcriptionally arrhythmic Arabidopsis TOC1-Ox plants as well as a *Neurospora* line that lacks a functional TTFL. The PRX over-oxidation rhythm even exists in cyanobacteria and archaea. Feeney *et al*, 2016 show that circadian magnesium ion transport can occur in transcriptionally inactive *Ostreococcus tauri* cells. Therefore, at least some eukaroytes possess an NTO which appears to have the same redox modification output and therefore may be evolutionarily ancient and conserved (Edgar *et al*, 2012).

In circadian biology, transcriptional studies have long dominated research efforts, leading to well-established TTFL models (e.g. Takahashi, 2016; Baker *et al*, 2012; Pokhilko *et al*, 2012; Fogelmark & Troein, 2014; Leloup & Goldbeter, 2003). However, it has become apparent that protein abundance and post-translational modification cannot be ignored, since these do not simply follow transcript expression patterns (e.g. Mauvoisin *et al*, 2013; Lück *et al*, 2014; Choudhary et al. 2016). With mass spectrometer technology becoming more and more advanced, several circadian proteomics studies have been conducted, such as proteomics analyses of protein abundance time courses (Robles *et al*, 2014; Reddy *et al*, 2006; Choudhary *et al*, 2016; Krahmer *et al*, 2018) or circadian phosphoproteomics (Robles *et al*, 2016; Choudhary *et al*, 2015).

In this study, we used mass spectrometry based proteomics and phosphoproteomics on circadian time courses to address the following questions: (1) How pervasive are rhythms in protein abundance and phosphorylation as a clock output in a normally functioning circadian clock system? and (2) can protein abundance or phosphorylation be rhythmic in a plant with a disabled transcriptional oscillator? To investigate (1), we used a time course of WT plants, and for addressing (2), we generated time courses of CCA1 overexpressing plants (CCA1-Ox), which are impaired in their TTFL. We generated global proteomics and phosphoproteomics data in parallel from the same protein extracts. Our analysis revealed that the transcriptional oscillator is required for most if not all rhythmic protein phosphorylation, and that most rhythmic phosphopeptides peak at subjective dawn. We also found this 'phospho-dawn' trend in the time courses with fluctuating phosphopeptides in the CCA1-Ox. Lastly, we selected one rhythmically changing phosphosite of the bifunctional enzyme fructose-6-phosphate-2-kinase / phosphatase (F2KP) and demonstrate that phospho mimetic mutation of the rhythmic site can have functional relevance.

Methods

Plant material

Col-0 and CCA1-OX (Wang & Tobin, 1998) *Arabidopsis thaliana* seeds (CCA1-Ox, Wang & Tobin, 1998) were used. Seeds were germinated and grown on plates (2.15g/l Murashige & Skoog medium

Basal Salt Mixture (Duchefa Biochemie), pH 5.8 (adjusted with KOH) and 12g/l agar (Sigma)) at 85µmol m^{-2} s^{-1} white fluorescent lights at 21°C in Percival incubators for 11 days in 12h light, 12h dark cycles. Seedlings were transferred to soil and grown for 11 more days at a light intensity of 110µmol m^{-2} s^{-1} in the same light-dark cycle pattern. At ZT0 of day 23, lights were switched to constant and harvesting was started 12h or 24h later in dataset I or dataset II, respectively. In dataset I, six time points at 4h intervals were taken with five replicates for each time point, harvesting eight rosettes for the WT and 12 rosettes for the CCA1-Ox. In dataset II, also at 4h intervals, at least six replicates of eight rosettes each were taken for the WT, five (16 rosettes each) of the CCA1-Ox. In dataset I, the time course was sampled from ZT12 to ZT32, in dataset II from ZT24 to 48 (WT) or ZT24 to ZT52 (CCA1-OX). Rosettes without roots were harvested by flash-freezing in liquid nitrogen.

Sample preparation

Protein extraction and precipitation was carried out according to method 'IGEPAL-TCA' in our previous publication (Krahmer *et al*, 2015). Briefly, protein was extracted and precipitated with TCA and phase separation, then washed with methanol and acetone. 500µg re-suspended protein was digested using a standard in-solution protocol and peptides were desalted. Before drying, the eluted peptides were separated into two parts: 490µg of the digest was used for phosphopeptide enrichment, 10µg was saved for global protein analysis. Phosphopeptides were enriched using the Titansphere™ spin tip kit (GL Sciences Inc.) and desalted on BondElut Omix tips (Agilent) according to the manufacturers' protocols.

Mass spectrometry, peptide merging and Progenesis analysis

LC-MS/MS measurement and subsequent analysis by the Progenesis software (version 4.1.4924.40586) was carried out as before (Krahmer *et al*, 2015): Dried peptides were dissolved in 12 µl or 20µl 0.05% TFA for phosphopeptide analysis, and global peptide analysis, respectively and passed through Millex-LH 0.45µm (Millipore) filters. 8 µl were run on an on-line capillary- HPLC-MSMS system consisting of a micropump (1200 binary HPLC system, Agilent, UK) coupled to a hybrid LTQ-Orbitrap XL instrument (Thermo-Fisher, UK). Reverse phase buffer used for LC-MS separation was buffer A (2.5% acetonitrile, 0.1% FA in H2O) and buffer B (10% H_2O, 90% acetonitrile, 0.1% formic acid, 0.025% TFA). LC peptide separation was carried out on an initial 80 min long linear gradient from 0% to 35% buffer B, then a steeper gradient up to 98% buffer B over a period of 20 min then remaining constant at 98% buffer B for 15 min until a quick drop to 0% buffer B before the end of the run at 120 min.

The tair Arabidopsis_1rep (version 20110103, 27416 protein entries) database was used for data-dependent detection, using the Mascot search engine (version 2.4), with including all peptide sequences of rank smaller than 5. Search parameters were as follows: charges 2+, 3+ and 4+, trypsin as enzyme, allowing up to two missed cleavages, carbamidomethyl (C) as a fixed modification, Oxidation (M), Phospho (ST) and Phospho (Y), Acetyl(Protein N-term) as variable modifications, a peptide tolerance of 7 ppm, and MS/MS tolerance of 0.4 Da, peptide charges 2+, 3+, and 4+, on an ESI-trap instrument, with decoy search and an ion-cutoff of 20. In all but one cases, these parameters resulted in a false-

discovery rate (FDR), of less than 5% (phospho I: 3.5%, phospho II: 3.2, global I: 6.8%, global II: 4.5%, calculated using the formula 2*d/(n+d) (Elias & Gygi, 2010), n and d being the number of hits in the normal and decoy databases, respectively, using an ion score cutoff of 20). Peptides were quantified by their peak area by Progenesis, and proteins were quantified by using the sum of the quantitation of all their unique peptides. Where peptides matched very similar proteins, multiple accession numbers are shown in exported results from Progenesis (supplementary data S1, S2).
In order to remove duplicates of phosphopeptides due to alternative modifications other than phosphorylation or missed cleavages, we used the qpMerge software following the Progenesis analysis (Hindle *et al*, 2016). The data are publicly available in the pep2pro database (Baerenfaller *et al*, 2011) at www.pep2pro.ethz.ch (Assembly names 'ed.ac.uk Global I', 'ed.ac.uk Global II', 'ed.ac.uk Phospho I', 'ed.ac.uk Phospho II') and have been deposited to the ProteomeXchange Consortium (http://proteomecentral.proteomexchange.org) via the PRIDE partner repository (Vizcaíno *et al*, 2014) with the dataset identifier PXD009230. Exported .csv files from Progenesis with all peptide and protein quantifications can be found in the online supplementary material (Data S1 and S2).

General statistics and outlier removal

Results of statistical analyses are summarised in data S3. Outlier analysis, statistics and Venn diagrams were done using R version 3.2.1 (R Core Team, 2015). Zero values for the quantification were exchanged for 'NA'. For outlier analysis and parametric tests such as ANOVA, arcsinh transformed data was used to obtain a normal distribution, while untransformed data was used for plotting time courses and for the non-parametric JTK_CYCLE analysis. For phosphoproteomics analysis all replicates in which the Pearson correlation coefficient among replicates of the same time point was lower than 0.8 were regarded as outliers (supplementary methods, supplementary data S4). In global dataset II, the first run replicate of each time point had to be excluded as an outlier due to an apparent drift (figure S13, S15). To generate heat maps, the abundance of each peptide or protein was normalized by the time course mean of the peptide or protein, followed by taking the log2 to centre values around 0, and the heatmap.2 function from the pvclust R package was applied (Suzuki & Shimodaira, 2015).

JTK_CYCLE analysis

We used the R-based tool JTK_CYCLE (Hughes *et al*, 2010) to determine rhythmicity, with the following modifications: (1) we ran the JTK_CYCLE algorithm for each phosphosite or protein separately rather than the entire list, to allow handling of missing quantification values for some replicates. Benjamini Hochberg (BH) (Benjamini & Hochberg, 1995) correction of p-values was carried out after application of the JTK_CYCLE tool. (2) Since our time course durations are close to the periods of rhythms we are searching for, some identifications were assessed as rhythmic by the original JTK_CYCLE tool that were increasing or decreasing continually over the entire time course. We excluded these from the group of rhythmic identifications. These continually rising or falling identifications were marked with 'excl.' in front of the p-value (supplementary data S5).

Kinase prediction using GPS3.0

Kinases for each site were predicted using the *Arabidopsis thaliana* specific GPS 3.0 prediction tool (Liu *et al*, 2015). For each phosphorylation site, an amino acid sequence was generated that contained 50 amino acids on either side of the phosphorylated residue using a python script. This resulted in 101 amino acid long sequences, unless the phosphosite was closer than 50 residues to the C or T terminus in which case the missing positions were filled by 'X'. The phosphopeptides used as foreground were the significantly rhythmic phosphosites (JTK_CYCLE p-value < 0.05) peaking at a given time point, all other phosphosites identified in the same experiment were used as background. The high threshold setting was used to minimize false-positive predictions and searches were done for S and T residues. In order to reduce the complexity of the dataset, we used a simplification: where kinases from different families were predicted, only the one with the highest difference between score and cutoff was used. For foreground and background the numbers of predictions for each occurring kinase group were counted and the Fisher's Exact test was used to determine predicted kinases that were significantly enriched in the foreground group ($p<0.05$).

GO analysis

For GO analysis, foreground and background were chosen as in the kinase prediction analysis. With these groups, GO analysis was conducted using the topGO script (Alexa *et al*, 2006), followed by Fisher's exact test to determine enrichment of terms (supplementary data S6).

Generation of F2KP point mutations and expression constructs

The F2KP coding sequence in the pDONR221 vector, lacking a stop codon, was kindly provided by Dr Sebastian Streb, ETH Zürich. The QuikChange Lightning Site-Directed Mutagenesis kit (Agilent Technologies) was used to introduce point mutations using primer pair AspF and AspR for mutation of S276 to aspartic acid or AlaF and AlaR for mutation to alanine (Table S 3). The F2KP coding sequence (the mutated constructs as well as the WT construct) was amplified by PCR using primers F2KP-F and F2KP-R (Table S 3), introducing restriction sites for AflII (3' end) and XbaI (5' end) and a stop codon. Using these restriction sites, digested PCR products were ligated into the pmcnEAVNG expression vector which allows expression in *E.coli* with an N-terminal GST tag and a T7 promoter for IPTG inducibility. Plasmids were transformed into Rosetta™2(DE3)pLysS Competent expression strain (Novagen).

Expression of GST-F2KP constructs in E. coli cells

The three constructs, WT, S276E and S276A were expressed in *E.coli* and purified using the GST tag. Two independent expression experiments were performed (experiment 1 and experiment 2), each in triplicates. 200ml *E.coli* cultures were grown at 37°C with 100µg/ml ampicillin and 25µg/ml chloramphenicol and induced with 1mM IPTG at OD_{600} values between 0.6 and 0.8. Cells were harvested by centrifugation after 2.5h of expression at 37°C. Each pellet was from 50ml bacterial culture. For purification of GST-F2KP, pellets were lysed in 2.5ml PBS with Complete protease inhibitor cocktail (Roche) with a probe sonicator. After clearing of the lysates, AP was carried out

using GSH-agarose beads, with 167µl GSH-agarose bead suspension (Protino glutathione agarose 4B, Macherey-Nagel), a binding incubation of 30min at room temperature, 4 washes with 10x the volume of the bead suspension and elution in PBS with 100mM reduced glutatione (pH 8.0) 3 times 30min at room temperature.

F2KP activity assay

F2KP activity of purified F2KP was measured as described in Kalt-Torres & Huber, 1987 (F-2,6-BP producing reaction) and Van Schaftingen *et al*, 1982 (measurement of generated F-2,6-BP by its activation of PFP and subsequent production of NADH produced from glycolytic enzymes).

Western blot quantification of F2KP concentration in AP eluates

To test whether the differences in F2KP activity of eluates could be caused by differences in abundance in the eluate, we quantified the amount of F2KP in equal volumes of eluates by western blotting.. Samples were prepared for SDS-PAGE with 25% 4xLDS (Life Technologies, NP0008) and 20mM DTT and were incubated at 70°C for 10min. Two concentration series of an equal mic of all three eluates were loaded on each gel for relative quantitation. Individual eluates were examined in duplicates (expression 1) or triplicates (expression 2). 4-12% Bis-Tris Gels (Life Technologies) were run and protein was blotted onto nitrocellulose membrane using the iBlot® system. Two primary antibodies were used in parallel: anti-F2KP from rabbit, raised against amino acids 566-651 (Villadsen & Nielsen, 2001) and anti-GST from mouse (Thermo Scientific), both at a dilution of 1:1,000 overnight. Secondary antibodies were goat-anti-rabbit (IRDye®800CW, LI-COR) and goat-anti-mouse (IRDye®680RD, LI-COR). Bands were quantified using the ImageStudioLite (version 2) software.

Results

Circadian protein phosphorylation requires the canonical transcriptional oscillator

We generated global proteomics and phosphoproteomics datasets for two independent circadian time courses and for two genotypes each – WT and the CCA1-Ox line which has an impaired circadian oscillator (Wang & Tobin, 1998). This resulted in four datasets: dataset I (Zeitgeber time (ZT) 12 to ZT32) and dataset II (ZT24 to ZT48 (CCA1-Ox) or ZT52 (WT)) (Figure 1). We removed outliers before conducting further stastical analysis as detailed in the methods section.

We identified 2287 phosphopeptides in dataset I, 1164 in dataset II, which condensed to between 1000 and 1500 in each dataset after applying qpMerge (Hindle *et al*, 2016) to remove duplicate phosphopeptides (Table 1 a). These were from several hundred proteins in each dataset and over 1000 in both datasets together (Table 1b). In the global protein analysis, we identified 1896 and 1340 proteins in dataset I and II, respectively, adding up to a total of 2501 for both datasets combined (Table 1a,b). To assess the circadian rhythmicity of each phosphopeptide or protein, we employed the non-parametric JTK_CYCLE tool (Hughes *et al*, 2010) as it can be applied to time courses of only one cycle, taking the curve shape into account. Unless otherwise stated we considered periods of 22 to 26h and excluded continuously increasing or decreasing profiles from the group of rhythmic

phosphopeptides or proteins. In dataset I, which started 12h earlier than dataset II, 606 (40%) phosphopeptides were rhythmic in the WT, in dataset II 100 (8.8%) when using p-values; 338 (23%) (dataset I) and 26 (2.3%) (dataset II) after carrying out p-value correction for multiple testing using the Benjamini-Hochberg method (Benjamini & Hochberg, 1995). The fraction of rhythmic proteins in the global proteomics analysis was smaller than in the case of phosphopeptides: 171 (9.0%) in dataset I, 45 (3.4%) in dataset II had JTK_CYCLE p-values < 0.05, 6 (0.32%) and (0.45%) with q-value < 0.05. Much fewer phosphopeptides and a similar number of global proteins were rhythmic in the CCA1-Ox, however after adjusting for multiple testing, no significant identifications remained apart from two phosphopeptides in dataset I (Table 1a).
As expected, the global analysis did not cover all proteins identified by phosphoproteomics (Figure 2a,c). We only found very few accessions with rhythms in protein as well as rhythmic phosphopeptides. About half of the rhythmic phosphopeptides or proteins also had rhythmic transcripts (Figure 2b,d).

'Phospho-dawn': most rhythmic phosphopeptides peak in the subjective morning
Analysis of the number of phosphopeptides that peak at each time point revealed that 45% (dataset I) and 73% (dataset II) of rhythmic phosphopeptides peak at subjective dawn in the WT (Figure 3, Figure 4a-b, Figure S 1a-b). This is in agreement with previous observations in Ostreococcus and Arabidopsis (Noordally *et al*, 2018; Choudhary *et al*, 2015). This trend to peak at dawn was not observed in the global proteomics dataset (Figure 3, Figure 4c-d, Figure S 1c-d) and is therefore most likely due to (de)phosphorylation events rather than protein abundance. Interestingly, when relaxing criteria for rhythmicity in the CCA1-Ox, by using p-values in stead of q-values, almost all rhythmic phosphopeptides peaked at subjective dawn. To expand the search for subjective dawn specific events in the CCA1-Ox, we tested whether there are rhythmic phosphopeptides with shorter periods in the CCA1-x (Figure 4e,f). We repeated the JTK_CYCLE analysis, allowing periods from 12 h to 26 h. As expected, hardly any phosphopeptides had periods of less than 22 h in the WT, while the majority of phosphopeptides had a predicted period of 12 or 16 h in the CCA1-Ox. Among those short-period rhythmic phosphopeptides, the majority of phosphopeptides peaked again at 24 h or 48 (Figure 4a,b). Since phospho dawn may not be completely abolished by impairment of the TTFL, we reasoned that there may be a kinase activity that is active in the subjective morning which is either very robustly dawn-timed, even when the TTFL is barely operating, or an alternative oscillator, possibly an NTO, contributes to the dawn phased kinase activity. Therefore, characterisation of these dawn-phased phosphopeptides could help to identify either a very robust dawn-phase TTFL output, or potentially even consequences of an NTO. We therefore focused on this group of phosphopeptides for further data analysis: GO analysis to search for common enriched functions of these phosphoproteins ; kinase prediction enrichment to obtain candidate kinases that may be involved in phospho dawn; and phosphosite motif analysis. In all these analyses we used the ZT24 or ZT48 peaking rhythmic (JTK_CYCLE p-value <0.05) phosphopeptides as foreground and all other identified phosphopeptides as background. As we used p-values instead of q-values in these analyses, we regard only those results that are supported by both datasets as reliable.

GO analysis

We analysed GO term enrichment on the phospho dawn group, and other time points where the foreground was sufficiently large (Table 3a,b, supplementary data S3). Only one GO term ('cotyledon development') was shared between the two phosphoproteomics datasets and the ZTs of enrichment are 16h apart (Table 3b). Several terms were shared between the WT and the CCA1-Ox (allowing shorter periods) in dataset I, most of them related to energy metabolism or ion homeostasis, and all of them were enriched at ZT24 or ZT28. Apart from overlap of exact GO IDs, we found enrichment of terms related to translation in the WT at 24h in both phosphoproteomics datasets, which is consistent with rhythmic phosphorylation of RPS6 (supplementary data S3, Choudhary *et al*, 2015)).

Kinase prediction and phosphorylation motif analysis

For predicting candidate kinases phosphorylating the subjective-dawn phased phosphopeptides, we used the software GPS3.0 (Liu *et al*, 2015) (Xue *et al*, 2008) because it offers a species-specific setting for *Arabidopsis thaliana*. We searched for enrichment of kinase groups among the rhythmic (JTK_CYCLE p-value <0.05,
Table 4) and also the significantly changing (ANOVA p-value<0.05, Table S 1) phosphopeptides. In the WT, both datasets share enrichment of CMGC kinase groups, in particular MAPK, as well as CAMK groups. The latter caught our attention since it is also enriched in the CCA1-Ox, particularly when allowing shorter periods. The CAMK group is the only consistently enriched group in the CCA1-Ox and also in the WT subjective dawn peaking group. On the EKPD database (Wang *et al*, 2014), used by GPS3, the CAMK group in plants contains the CDPK/SnRK family of kinases with 89 members (Hrabak *et al*, 2003). Among the phospho dawn peptides we found known (direct or indirect) SnRK1 targets (Figure 5, Table S 2). To complement the GPS3.0 analysis, we searched for the SnRK1 target pattern, firstly with hydrophobic amino acids at the -5 and +4 positions (Broeckx *et al*, 2016) (supplementary methods) and found significant enrichment in the phosphopeptides peaking at ZT24 in dataset II, allowing periods between 22 and 26h in the CCA1-Ox (Table S 4). However when including the requirement for a basic amino acid at position -4 or -3 (Sugden *et al*, 1999) the number of sequences identified in foreground and the background was too low for meaningful statistical analysis. We generated target site motifs using the pLogo tool (O'Shea *et al*, 2013) (supplementary methods, Figure S2, Figure S3). The only significantly enriched position in the WT was D at the +1 (dataset I). In the CCA1-Ox, a D was significantly enriched at the -5 position in dataset I, as well as Ms at the +1 or -6 positions and a V at -2 in dataset II. However, none of these over-representations were consistent between datasets (Figure S 2, Figure S 3).

Rhythmically phosphorylated kinases and phosphatases

Since kinases and phosphatases themselves can be regulated by phosphorylation, we were interested in rhythmic phosphopeptides of kinases and phosphatases. Identification of rhythmic kinase or phosphatase activities in the WT could therefore help to discover new clock output pathways via protein phosphorylation, as a consequence of normal clock function, or components of an NTO.

For two kinases, CRK8 and AT5G61560, we found rhythmic phosphopeptides in the WT with non-changing protein abundance, indicating that rhythmicity is due to phosphorylation rather than changes in protein abundance (Figure 6a,b). CRK8 is a member of the CDPK-SnRK1 superfamily (Hrabak *et al*, 2003).

All rhythmically phosphorylated phosphatases in our data are members of the protein phosphatase 2 C (PP2C) family (Figure 7) and they are rhythmic only in the WT. Some PP2Cs can dephosphorylate and inactivate SnRK1 (Rodrigues *et al*, 2013) and may therefore also play a role in phospho dawn.

For most of the kinases and phosphatases shown here, the CCA1-Ox vaguely follows the WT pattern, but it is not classified as rhythmic by JTK_CYCLE (with the exception of At5g14720, Figure 6d), therefore these phosphorylation events are likely to be an output of the TTFL.

Functions of rhythmic phosphoproteins in the WT include transport, regulation of translation, photosynthesis, carbon and nitrogen metabolism

Phosphoproteins that were rhythmic in the WT are associated with a variety of physiological functions (Table 2, supplementary data S2). EIF4G, RPS6A and RPS6B are involved in translation initiation (Schepetilnikov *et al*, 2013; Jackson *et al*, 2010)(Choudhary *et al*, 2015). CINV1 is required for carbon metabolism and growth (Barratt *et al*, 2009), SWEET12 facilitates sucrose transport (Chen *et al*, 2012). NIA2, the transporter NRT1.7, the nitrate transporter and sensor CLC-A, the ammonium transporter AMT1;1 and ASN2 are all involved in nitrogen and / or amino acid metabolism (Wilkinson & Crawford, 1991; Fan *et al*, 2009; Ho *et al*, 2009; Ninnemann *et al*, 1994; Gaufichon *et al*, 2013). CAB4 is a light harvesting complex component (Zhang *et al*, 1991), while COL9 is clock regulated and involved in flowering (Cheng & Wang, 2005). DDB1-CUL4 is an E3 ubiquitin ligase (Zhang *et al*, 2008), PIP3 is an aquaporin (Weig *et al*, 1997).

Only few proteins are rhythmically phosphorylated in the CCA1-Ox in both datasets

The overlap of rhythmic phosphopeptides between datasets for the CCA1-Ox is small (Table 1, Table 2). With 22 to 26h periods, phosphopeptides of a Leucine rich repeat protein kinase as well as Dormany/auxin associated family protein are shared, though the latter also showed a significant increase in its protein abundance in dataset I (supplementary data S2) in the CCA1-Ox, therefore changes may be due to increasing protein expression in constant light. When allowing shorter periods, NIA1 as well as a remorin family protein were rhythmic.

Circadian rhythms in protein abundance in the global proteomics datasets

We applied the same rhythmicity, peak time distribution and GO analyses to the global proteomics data (Table 3c,d, supplementary data 3). In both datasets, enriched GO terms in the WT at the end of the subjective day (ZT12 and ZT36) were photosynthesis related terms, ‘response to glucose’, ‘regulation of protein dephosphorylation’ and an oxidoreductase activity with NAD or NADP as acceptor. The latter was also enriched in the CCA1-Ox in dataset I (Table 3d). In the CCA1-Ox, two terms related to cell wall metabolic processes were enriched in both datasets during the subjective night (ZT20 and ZT44) (Table 3d). Looking at individual rhythmic proteins shared between the datasets, we identified

six for he WT, three for the CCA1-Ox (Table 2d,e). One protein, INOSITOL 3- PHOSPHATE SYNTHASE 1 (MIPS1, AT4G39800) was rhythmic in both datasets and both genotypes.
Among the non-shared rhythmic proteins in the WT were several ribosomal proteins and proteins of the photosynthetic machinery (supplementary data 2), in agreement with published data (Choudhary *et al*, 2015).

F2KP is rhythmically phosphorylated at the conserved residue Ser276
As an example of how our datasets can be used to investigate new clock output pathways, we analysed the molecular function of a rhythmic phosphosite in the bifunctional enzyme F2KP. Several phosphosites were detected in F2KP with only S276 showing a circadian rhythm in the WT in dataset II (Figure 5d). Only one F2KP peptide was detected in the global protein analysis and only in dataset II. Since its changes over time are not significant and not in phase with the phosphopeptide including S276 it is unlikely that the rhythm in S276 phosphorylation is caused by changes in F2KP protein abundance.

Point mutation of S276 affects F2KP kinase activity in vitro
To test if the S276 phosphorylation site is functionally relevant, we measured the maximum F6P,2K activity of phosphomimetic mutants S276D and S276A with the unmutated WT control enzyme *in vitro*. Two independent expressions and subsequent purifications using a GST tag were carried out to ensure reproducibility. S276A had an approximately 2.5 fold increased activity compared to the unmutated version, while S276D had only slightly increased activity, which was statistically significant in one out of two independent experiments (Figure 9a,b, Figure S5a,b,d). Equivalent amount of expressed F2KP protein in assays was verified by western blotting (Figure 9, Figure S5) with two different antibodies (Figure 9c, Figure S5c).

Discussion
In this study, we generated and analysed global and phospho- proteomics time courses for two mains reasons: Firstly, by studying WT plants in constant conditions, we aimed to find out how pervasive rhythmicity of protein phosphorylation and abundance is in constant conditions and a normally functioning clock; this also involved identification of rhythmic proteins / phosphorylation events and could allow discovery of novel clock output pathways through protein phosphorylation. Secondly, by applying the same approach to the CCA1-Ox line, we aimed to identify candidate processes, proteins and phosphorylation events that are rhythmic in spite of an impaired transcriptional oscillator, and may therefore be driven by an NTO.

Rhythmic protein phosphorylation is more wide-spread than rhythmic protein abundance
According to our data (Table 1), the proportion of rhythmic phosphopeptides is larger than for proteins, but smaller than for rhythmic transcripts (Covington *et al*, 2008). The fact that the proportion of rhythmic identifications is higher in dataset I than in dataset II is likely due to dampening of rhythms in the later sampled dataset II. In the CCA1-Ox, some rhythmic phosphopeptides were detected,

however amplitudes were lower than in the WT and most changing phosphopeptides had a shorter, and therefore not circadian period.

We found rhythmic phosphorylation of proteins related to a variety of processes in the WT, many of which are in agreement with a previous study (Choudhary *et al*, 2015), such as proteins involved in nitrogen metabolism and translation. GO analysis of our phosphoproteomics data also suggests circadian rhythmicity of ion transport or homeostasis related processes in the WT at subjective dawn, in agreement with rhythms of calcium ion concentration in Arabidopsis (Xu *et al*, 2007) and magnesium ions in *Ostreococcus* and other organisms (Feeney *et al*, 2016). GO analysis for the global protein data confirmed enrichment of photosynthesis related terms (Choudhary *et al*, 2016). Of particular interest is also the enrichment of oxidoreductase activity with NAD or NADP as acceptors, and protein dephosphorylation processes at subjective dusk.

Identification of candidate protein kinases involved in phospho-dawn

Our kinase prediction and enrichment analysis revealed enrichment of some CMGC subgroups, such as MAPK, CK2, GSK, DYRK, CDK or DAPK. CK2 is involved in the circadian clock function in Arabidopsis by phosphorylating CCA1 (Sugano *et al*, 1999; Daniel *et al*, 2004). A previous study reported enrichment of predominantly CK2 predictions among significantly changing phosphopeptides, though usage of the whole genome as enrichment background may have introduced a bias for highly abundant kinases and targets (Choudhary *et al*, 2015). Roles for MAPK and GSK have been reported for the circadian clock function in other eukaryotes (Akashi & Nishida, 2000; Iitaka *et al*, 2005; Besing *et al*, 2015; Martinek *et al*, 2001). Our kinase prediction analysis focused on the phospho-dawn peptides where the most consistent enrichment – at both dawn time points, in both datasets, and both genotypes – was for CAMK groups. On the database EKPD, which GPS3.0 is based on, the CAMK group in plants comprises 89 members of the CDPK-SnRK superfamily of kinases.

SnRK1 as a candidate protein kinase for phospho-dawn

Even though all of these 89 CDPK-SnRK member are potential candidates, SnRK1 appeared the most plausible one for three main reasons. Firstly, relevance of SnRK1 in circadian timing has previously been reported: SnRK1 genetically interacts with the clock protein TIC (Sánchez-Villarreal *et al*, 2018), affects circadian period in the light (Shin *et al*, 2017), and is involved in entrainment to sugar (Frank *et al*, 2018). Secondly, SnRK1 is an important metabolic hub, and in normal light-dark conditions the morning is associated with profound metabolic changes in plants, such as transition from using starch to direct photoassimilates, but also transition from normal starch usage to a starvation response if light intensities are low in the morning but starch is alomost depleted. Thirdly, among the phospho dawn phosphosites are known, rather than just predicted SnRK1 targets and interactors. Targets include F2KP, sucrose phosphate synthase and nitrate reductases NIA1 and NIA2 (Figure 5). In addition, PP2Cs which may regulate SnRK1 have phosphosites that peak at subjective dawn (Woods *et al*, 2003; Rodrigues *et al*, 2013). DUF581 interacts with SnRK1 and serves as platform for SnRK1 signalling (Nietzsche *et al*, 2014). DUF581 protein abundance was rhythmic in global dataset I (not detected in

dataset II), one phosphopeptide was rhythmic in the WT in both datasets and in the CCA1-Ox in dataset I (Table 2 and supplementary data S2).

Interestingly, SnRK1 signaling is regarded as antagonistic to TOR signaling (Nukarinen *et al*, 2016) but both RPS6A and RPS6B, ribosomal proteins and TOR targets, are rhythmically phosphorylated in the WT, and in dataset I also in the CCA1-Ox (supplementary data S2), with their phosphorylation peaks at subjective dawn, confirming published data (Choudhary *et al*, 2015). This indicates that the interplay between SnRK1 and TOR may be more complex than simply antagonistic.

Could an NTO contribute to phospho-dawn?

Since the Kai proteins are not found in eurkaryotes, they cannot be the drivers of eukaryotic clocks. However, the fact that KaiC autophosphorylation creates 24h rhythms in a test tubes shows that it is biochemically possible phosphorylation reactions to drive circadian rhytms. In addition, since kinases exist that are involved in clocks across kingdoms, phosphorylation in circadian timing may be more conserved than the actual clock genes. The conserved kinases are therefore candidates for NTO components or links between the NTO and the TTFL. For these reason, we hypothesized that protein phosphorylation could be involved in a plant NTO mechanism. We used the CCA1-Ox as an approximation of a plant without a functional canonical TTFL. We cannot fully exclude a remaining low amplitude canonical TTFL, or an alternative transcriptional oscillator operation in the CCA1-Ox since transcriptomics studies in this line have not been published. However, simulation of increased CCA1 levels with the Arabidopsis clock model predicts period lengthening (data not shown), while with the relaxed JTK_CYCLE p-value < 0.05 (rather than q-value) we observe either approximately 24h or shorter periods in this line. Therefore, there may be room for speculations that either the TTFL has an extremely robust metabolic or protein kinase activity output at subjective dawn even if otherwise severely impaired, or that an NTO gives a time cue that has a small contribution to phospho dawn. It did not escape our attention that indeed some properties of SnRK1, or related protein kinases, would make them good candidates for NTO components, given likely conservation of the NTO and parallels to the cyanobacterial NTO. For example, SnRK1 is conserved with animals and fungi (Polge & Thomas, 2007; Hrabak *et al*, 2003), with AMPK being involved in circadian timing in mammals (Lamia *et al*, 2009). In addition, the activating kinases of SnRK1, SnAK1 and SnAK2 (Crozet *et al*, 2010) and other members of the family auto-phosphorylate, some of them very slowly, like KaiC (Oh *et al*, 2012; Iwasaki *et al*, 2002; Nemoto *et al*, 2015). Like AMPK (Oakhill *et al*, 2011; Gowans *et al*, 2013) and SNF-1 (Mayer *et al*, 2011), SnRK1 is regulated by adenylates as it is protected by AMP from dephosphorylation by PP2C *in vitro* (Sugden *et al*, 1999) and interacts with adenosine kinase (Mohannath *et al*, 2014). Adenylates have previously been suggested as NTO components in an alga (Goto *et al*, 1985). In summary, even though the preservation of the phospho-dawn and its predicted kinases in the CCA1-Ox and WT are intriguing, we did not find overwhelming evidence for genuinely rhythmic phosphopeptides and the existence of an NTO in the CCA1-Ox.

Phosphomimetic studies illustrate how datasets can be used to discover novel clock output pathways
The specific roles of most of the rhythmic phosphorylation sites identified in our study have not been investigated. To link circadian phosphorylation of a protein to its function, we analysed the effect of a phosphosite of the enzyme F2KP on its activity using phosphomimetic mutations *in vitro*. F2KP is one of the regulators of carbon partitioning into starch and sucrose (Nielsen *et al*, 2004) and is necessary to maintain normal growth in fluctuating light conditions (McCormick & Kruger, 2015).
The phosphosite of interest, S276, is within the plant-specific regulatory N-terminal domain (Villadsen *et al*, 2000; Villadsen & Nielsen, 2001) but is not among the phosphosites in the 14-3-3 binding site (Kulma *et al*, 2004). S276 is also a likely SnRK1 target (Cho *et al*, 2016), even though it lacks a typical SnRK1 target pattern. S276 is conserved in many plant species or replaced by a threonine residue (Figure S 4). Our *in-vitro* phosphomimetic experiments suggest that a lack of negative charge at position 276 increases F2KP's kinase activity. F-2,6-BP levels in the plant increase slowly across the day in short day conditions (Kulma *et al*, 2004). Since F2KP is the only enzyme that converts between F-2,6-BP and F-6-P, F2KP activity must gradually increase during the day. Our results suggest that S276 phosphorylation could be responsible as S276 phosphorylation decreases during the day, as out measurements suggest, increases its activity. This would favour channeling of carbon into starch more at the end of the day than in the morning. Since starch builds up at a fairly constant rate across the day (Smith *et al*, 2004), this does not appear to translate directly into increasing carbon fluxes into starch. Rather, we hypothesize that F2KP regulation may play together with other regulators of carbon partitioning and may be more relevant in fluctuating than constant light, where it is important for growth (McCormick & Kruger, 2015), for example to guarantee sufficient carbon supply for sucrose formation in the morning but prioritizing building up of starch resources toward the end of the day.

In conclusion, we have demonstrated how these phosphoproteomics datasets can be used to explore new circadian clock output pathways.

References

Akashi M & Nishida E (2000) Involvement of the MAP kinase cascade in resetting of the mammalian circadian clock. Genes Dev. 14: 645–649

Alexa A, Rahnenführer J & Lengauer T (2006) Improved scoring of functional groups from gene expression data by decorrelating GO graph structure. Bioinformatics 22: 1600–7

Baerenfaller K, Hirsch-Hoffmann M, Svozil J, Hull R, Russenberger D, Bischof S, Lu Q, Gruissem W & Baginsky S (2011) pep2pro: a new tool for comprehensive proteome data analysis to reveal information about organ-specific proteomes in Arabidopsis thaliana. Integr. Biol. (Camb). 3: 225–37

Baker CL, Loros JJ & Dunlap JC (2012) The circadian clock of Neurospora crassa. FEMS Microbiol. Rev. 36: 95–110

Barratt DHP, Derbyshire P, Findlay K, Pike M, Wellner N, Lunn J, Feil R, Simpson C, Maule AJ & Smith AM (2009) Normal growth of Arabidopsis requires cytosolic invertase but not sucrose synthase. PNAS 106: 13124–13129

Benjamini Y & Hochberg Y (1995) Controlling the False Discovery Rate : A Practical and Powerful Approach to Multiple Testing. J R Stat. Soc B 57: 289–300

Besing RC, Paul JR, Hablitz LM, Rogers CO, Johnson RL, Young ME & Gamble KL (2015) Circadian Rhythmicity of Active GSK3 Isoforms Modulates Molecular Clock Gene Rhythms in the Suprachiasmatic Nucleus. J. Biol. Rhythms

Broeckx T, Hulsmans S & Rolland F (2016) The plant energy sensor: evolutionary conservation and divergence of SnRK1 structure, regulation, and function. J. Exp. Bot. 67: 6215–6252

Chen L-Q, Qu X-Q, Hou B-H, Sosso D, Osorio S, Fernie AR & Frommer WB (2012) Sucrose Efflux Mediated by SWEET Proteins as a Key Step for Phloem Transport. Science 335: 207–211

Cheng X-F & Wang Z-Y (2005) Overexpression of COL9, a CONSTANS-LIKE gene, delays flowering by reducing expression of CO and FT in Arabidopsis thaliana. Plant J. 43: 758–68

Cho HY, Wen TN, Wang YT & Shih MC (2016) Quantitative phosphoproteomics of protein kinase SnRK1 regulated protein phosphorylation in Arabidopsis under submergence. J. Exp. Bot. 67: 2745–2760

Choudhary MK, Nomura Y, Shi H, Nakagami H & Somers DE (2016) Circadian Profiling of the Arabidopsis Proteome Using 2D-DIGE. Front. Plant Sci. 7: 1–14

Choudhary MK, Nomura Y, Wang L, Najagami H & Somers DE (2015) Quantitative circadian phosphoproteomic analysis of Arabidopsis reveals extensive clock control of key components in physiological, metabolic and signaling pathways. Mol. Cell. Proteomics 14: 2243–2260

Covington MF, Maloof JN, Straume M, Kay S a & Harmer SL (2008) Global transcriptome analysis reveals circadian regulation of key pathways in plant growth and development. Genome Biol. 9: R130

Crozet P, Jammes F, Valot B, Ambard-Bretteville F, Nessler S, Hodges M, Vidal J & Thomas M (2010) Cross-phosphorylation between Arabidopsis thaliana sucrose nonfermenting 1-related protein kinase 1 (AtSnRK1) and its activating kinase (AtSnAK) determines their catalytic activities. J. Biol. Chem. 285: 12071–12077

Daniel X, Sugano S & Tobin EM (2004) CK2 phosphorylation of CCA1 is necessary for its circadian oscillator function in Arabidopsis. Proc. Natl. Acad. Sci. U. S. A. 101: 3292–7

Edgar RS, Green EW, Zhao Y, van Ooijen G, Olmedo M, Qin X, Xu Y, Pan M, Valekunja U, Feeney KA, Maywood ES, Hastings MH, Baliga NS, Merrow M, Millar AJ, Johnson CH, Kyriacou CP, O'Neill JS & Reddy AB (2012) Peroxiredoxins are conserved markers of circadian rhythms. Nature

Elias JE & Gygi SP (2010) Target-Decoy Search Strategy for Mass. Methods Mol. Biol. 604: 55–71

Fan S, Lin C, Hsu P, Lin S & Tsay Y (2009) The Arabidopsis Nitrate Transporter NRT1 . 7 , Expressed in Phloem, Is Responsible for Source-to-Sink Remobilization of Nitrate. Plant Cell 21: 2750–2761

Feeney KA, Hansen LL, Putker M, Olivares-Yanez C, Day J, Eades LJ, Larrondo LF, Hoyle NP, O'Neill JS & van Ooijen G (2016) Daily magnesium fluxes regulate cellular timekeeping and energy balance. Nature 532: 375–379

Fogelmark K & Troein C (2014) Rethinking Transcriptional Activation in the Arabidopsis Circadian Clock. PLoS Comput. Biol. 10: e1003705

Frank A, Matiolli CC, Viana AJC, Hearn TJ, Kusakina J, Belbin FE, Wells Newman D, Yochikawa A, Cano-Ramirez DL, Chembath A, Cragg-Barber K, Haydon MJ, Hotta CT, Vincentz M, Webb AAR & Dodd AN (2018) Circadian Entrainment in Arabidopsis by the Sugar-Responsive Transcription Factor bZIP63. Curr. Biol. 28: 2597-2606.e6

Gaufichon L, Masclaux-daubresse C, Tcherkez G, Reisdorf-cren M, Sakakibara Y, Hase T, Clément G, Avice J, Grandjean O, Marmagne A, Boutet-mercey S, Azzopardi M, Soulay F & Suzuki A (2013) Arabidopsis thaliana ASN2 encoding asparagine synthetase is involved in

the control of nitrogen assimilation and export during vegetative growth. Plant, Cell Environ. 36: 328–342

Goto K, Laval-Martin L & Edmunds LN (1985) Biochemical Modeling of an Autonomously Oscillatory Circadian Clock in Euglena. Science 228: 1284–1288

Gowans GJ, Hawley SA, Ross FA & Hardie DG (2013) AMP is a true physiological regulator of amp-activated protein kinase by both allosteric activation and enhancing net phosphorylation. Cell Metab. 18: 556–566

Hindle MM, Le Bihan T, Krahmer J, Martin SF, Noordally ZB, Simpson TI & Millar AJ (2016) qpMerge: Merging different peptide isoforms using a motif centric strategy. bioRxiv 047100

Ho CH, Lin SH, Hu HC & Tsay YF (2009) CHL1 Functions as a Nitrate Sensor in Plants. Cell 138: 1184–1194

Hrabak EM, Chan CWM, Gribskov M, Harper JF, Choi JH, Halford N, Luan S, Nimmo HG, Sussman MR, Thomas M, Walker-simmons K, Zhu J & Harmon AC (2003) The Arabidopsis CDPK-SnRK Superfamily of Protein Kinases. Plant Physiol. 132: 666–680

Hughes ME, Hogenesch JB & Kornacker K (2010) JTK_CYCLE: An Efficient Nonparametric Algorithm for Detecting Rhythmic Components in Genome-Scale Data Sets. J. Biol. Rhythms 25: 372–380

Iitaka C, Miyazaki K, Akaike T & Ishida N (2005) A role for glycogen synthase kinase-3beta in the mammalian circadian clock. J. Biol. Chem. 280: 29397–29402

Iwasaki H, Nishiwaki T, Kitayama Y, Nakajima M & Kondo T (2002) KaiA-stimulated KaiC phosphorylation in circadian timing loops in cyanobacteria. Proc. Natl. Acad. Sci. U. S. A. 99: 15788–15793

Jackson RJ, Hellen CUT & Pestova T V (2010) The mechanism of eukaryotic translation initiation and principles of its regulation. Nat. Rev. Mol. Cell Biol. 11: 113–127

Kalt-Torres W & Huber SC (1987) Diurnal Changes in Maize Leaf Photosynthesis. Plant Physiol. 83: 283–288

Krahmer J, Goralogia GS, Kubota A, Zardilis A, Johnson RS, Song YH, MacCoss MJ, LeBihan T, Halliday KJ, Imaizumi T & Millar AJ (2018) Time-resolved Interaction Proteomics of the GIGANTEA Protein Under Diurnal Cycles in Arabidopsis. FEBS Lett.: 1873-3468.13311

Krahmer J, Hindle MM, Martin SF, Bihan T Le & Millar AJ (2015) Sample Preparation for Phosphoproteomic Analysis of Circadian Time Series in Arabidopsis thaliana. In Circadian Rhythms and Biological Clocks pp 405–431. Elsevier Inc.

Kulma A, Villadsen D, Campbell DG, Meek SEM, Harthill JE, Nielsen TH & MacKintosh C (2004) Phosphorylation and 14-3-3 binding of Arabidopsis 6-phosphofructo-2-kinase/fructose-2,6-bisphosphatase. Plant J. 37: 654–667

Kusakina J & Dodd AN (2012) Phosphorylation in the plant circadian system. Trends Plant Sci.: 1–9

Lamia KA, Sachdeva UM, Ditacchio L, Williams EC, Alvarez JG, Egan DF, Vasquez DS, Juguilon H, Panda S, Shaw RJ, Thompson CB & Evans RM (2009) AMPK Regulates the Circadian Clock by Cryptochrome Phosphorylation and Degradation. Science 326: 437–441

Leloup JC & Goldbeter A (2003) Toward a detailed computational model for the mammalian circadian clock. Proc Natl Acad Sci U S A 100: 7051–7056

Liu Z, Wang Y, Cheng H, Deng W, Pan Z, Ullah S, Ren J & Xue Y (2015) GPS 3.0: web servers for the prediction of protein post-translational modification sites. Manuscr. Submitt.

Lück S, Thurley K, Thaben PF & Westermark PO (2014) Rhythmic Degradation Explains and Unifies Circadian Transcriptome and Proteome Data. Cell Rep.: 741–751

Maier B, Wendt S, Vanselow JT, Wallach T, Reischl S, Oehmke S, Schlosser A & Kramer A (2009) A large-scale functional RNAi screen reveals a role for CK2 in the mammalian circadian clock. Genes Dev. 23: 708–718

Martinek S, Inonog S, Manoukian AS & Young MW (2001) A role for the segment polarity gene shaggy/GSK-3 in the Drosophila circadian clock. Cell 105: 769–779

Mauvoisin D, Wang J, Jouffe C, Martin E, Atger F, Waridel P, Quadroni M, Gachon F & Naef F (2013) Circadian clock-dependent and -independent rhythmic proteomes implement distinct diurnal functions in mouse liver. Proc. Natl. Acad. Sci. U. S. A.

Mayer F V., Heath R, Underwood E, Sanders MJ, Carmena D, McCartney RR, Leiper FC, Xiao B, Jing C, Walker PA, Haire LF, Ogrodowicz R, Martin SR, Schmidt MC, Gamblin SJ & Carling D (2011) ADP regulates SNF1, the saccharomyces cerevisiae homolog of AMP-activated protein kinase. Cell Metab. 14: 707–714

McCormick AJ & Kruger NJ (2015) Lack of fructose 2,6-bisphosphate compromises photosynthesis and growth in Arabidopsis in fluctuating environments. Plant J.

Mohannath G, Jackel JN, Lee YH, Buchmann RC, Wang H, Patil V, Adams AK & Bisaro DM (2014) A complex containing SNF1-related kinase (SnRK1) and adenosine kinase in arabidopsis. PLoS One 9:

Nakajima M, Imai K, Ito H, Nishiwaki T, Murayama Y, Iwasaki H, Oyama T & Kondo T (2005) Reconstitution of circadian oscillation of cyanobacterial KaiC phosphorylation in vitro. Science 308: 414–5

Nemoto K, Takemori N, Seki M, Shinozaki K & Sawasaki T (2015) Members of the Plant CRK-superfamily are Capable of trans-/auto-Phosphorylation of Tyrosine Residues. J. Biol. Chem.: jbc.M114.617274

Nielsen TH, Rung JH & Villadsen D (2004) Fructose-2,6-bisphosphate: a traffic signal in plant metabolism. Trends Plant Sci. 9: 556–63

Nietzsche M, Schießl I & Börnke F (2014) The complex becomes more complex: protein-protein interactions of SnRK1 with DUF581 family proteins provide a framework for cell- and stimulus type-specific SnRK1 signaling in plants. Front. Plant Sci. 5: 54

Ninnemann O, Jauniaux JC & Frommer WB (1994) Identification of a high affinity NH4+ transporter from plants. EMBO J. 13: 3464–3471

Nishiwaki T, Satomi Y, Nakajima M, Lee C, Kiyohara R, Kageyama H, Kitayama Y, Temamoto M, Yamaguchi A, Hijikata A, Go M, Iwasaki H, Takao T & Kondo T (2004) Role of KaiC phosphorylation in the circadian clock system of Synechococcus elongatus PCC 7942. PNAS 101: 13927–13932

Noordally ZB, Hindle MM, Martin SF, Seaton D, Simpson I, Le Bihan T & Millar AJ (2018) Circadian protein regulation in the green lineage I. A phospho-dawn anticipates light onset before proteins peak in daytime. bioRxiv: http://dx.doi.org/10.1101/287862

Nukarinen E, Nägele T, Pedrotti L, Wurzinger B, Mair A, Landgraf R, Börnke F, Hanson J, Teige M, Baena-Gonzalez E, Dröge-Laser W & Weckwerth W (2016) Quantitative phosphoproteomics reveals the role of the AMPK plant ortholog SnRK1 as a metabolic master regulator under energy deprivation. Sci. Rep. 6: 31697

O'Neill JS, van Ooijen G, Dixon LE, Troein C, Corellou F, Bouget F-Y, Reddy AB & Millar AJ (2011) Circadian rhythms persist without transcription in a eukaryote. Nature 469: 554–8

O'Neill JS & Reddy AB (2011) Circadian clocks in human red blood cells. Nature 469: 498–503

O'Shea JP, Chou MF, Quader S a, Ryan JK, Church GM & Schwartz D (2013) pLogo: a probabilistic approach to visualizing sequence motifs. Nat. Methods 10: 1211–2

Oakhill JS, Steel R, Chen Z, Scott JW, Ling N, Tam S & Kemp BE (2011) AMPK is a direct adenylate charge-regulated protein kinase. Science 2857: 1433–1435

Oh MH, Wu X, Kim HS, Harper JF, Zielinski RE, Clouse SD & Huber SC (2012) CDPKs are dual-specificity protein kinases and tyrosine autophosphorylation attenuates kinase activity. FEBS Lett. 586: 4070–4075

van Ooijen G & Millar AJ (2012) Non-transcriptional oscillators in circadian timekeeping. Trends Biochem. Sci. 37: 484–92

Pokhilko A, Fernández AP, Edwards KD, Southern MM, Halliday KJ & Millar AJ (2012) The clock gene circuit in Arabidopsis includes a repressilator with additional feedback loops. Mol. Syst. Biol. 8: 574

Polge C & Thomas M (2007) SNF1 AMPK SnRK1 kinases, global regulators at the heart of energy control? Trends Plant Sci. 12: 20–28

R Core Team (2015) R: A Language and Environment for Statistical Computing.

Reddy AB, Karp N a, Maywood ES, Sage E a, Deery M, O'Neill JS, Wong GKY, Chesham J, Odell M, Lilley KS, Kyriacou CP & Hastings MH (2006) Circadian orchestration of the hepatic proteome. Curr. Biol. 16: 1107–15

Robles MS, Cox J & Mann M (2014) In-Vivo Quantitative Proteomics Reveals a Key Contribution of Post-Transcriptional Mechanisms to the Circadian Regulation of Liver Metabolism. PLoS Genet. 10:

Robles MS, Humphrey SJ, Mann M, Altelaar AF, Munoz J, Heck AJ, Baker CL, Kettenbach AN, Loros JJ, Gerber SA, Dunlap JC, Bugge A, Feng D, Everett LJ, Briggs ER, Mullican SE, Wang F, Jager J, Lazar MA, Chen W, et al (2016) Phosphorylation Is a Central Mechanism for Circadian Control of Metabolism and Physiology. Cell Metab. 0: 35–48

Rodrigues A, Adamo M, Crozet P, Margalha L, Confraria A, Martinho C, Elias A, Rabissi A, Lumbreras V, González-Guzmán M, Antoni R, Rodriguez PL & Baena-González E (2013) ABI1 and PP2CA phosphatases are negative regulators of Snf1-related protein kinase1 signaling in Arabidopsis. Plant Cell 25: 3871–84

Sánchez-Villarreal A, Davis AM & Davis SJ (2018) AKIN10 activity as a cellular link between metabolism and circadian-clock entrainment in Arabidopsis thaliana. Plant Signal. Behav. 13: e1411448

Van Schaftingen E, Lederer B, Bartrons R & Hers H-G (1982) A Kinetic Study of Pyrophosphate : Fructose-6-Phosphate Phosphotransferase from Potato Tubers Application to a Microassay of Fructose 2,6-Bisphosphate. Eur. J. Biochem. 129: 191–195

Schepetilnikov M, Dimitrova M, Mancera-Martínez E, Geldreich A, Keller M & Ryabova LA (2013) TOR and S6K1 promote translation reinitiation of uORF-containing mRNAs via phosphorylation of eIF3h. EMBO J. 32: 1087–102

Shin J, Sánchez-Villarreal A, Davis AM, Du S, Berendzen KW, Koncz C, Ding Z, Li C & Davis SJ (2017) The metabolic sensor AKIN10 modulates the Arabidopsis circadian clock in a light-dependent manner. Plant. Cell Environ.

Smith S, Fulton D, Chia T, Thorneycroft D, Chapple a, Dunstan H, Hylton C, Zeeman S & Smith a (2004) Diurnal changes in the transcriptome encoding enzymes of starch metabolism provide evidence for both transcriptional and posttranscriptional regulation of starch metabolism in arabidopsis leaves. Plant Physiol. 136: 2687–2699

Sugano S, Andronis C, Ong MS, Green RM & Tobin EM (1999) The protein kinase CK2 is involved in regulation of circadian rhythms in Arabidopsis. PNAS 96: 12362–6

Sugden C, Donaghy PG, Halford NG & Hardie DG (1999) Two SNF1-related protein kinases from spinach leaf phosphorylate and inactivate 3-hydroxy-3-methylglutaryl-coenzyme A reductase, nitrate reductase, and sucrose phosphate synthase in vitro. Plant Physiol 120: 257–274

Suzuki R & Shimodaira H (2015) pvclust: Hierarchical Clustering with P-Values via Multiscale Bootstrap Resampling.

Takahashi JS (2016) Transcriptional architecture of the mammalian circadian clock. Nat. Rev. Genet.

Villadsen D & Nielsen TH (2001) N-terminal truncation affects the kinetics and structure of fructose-6-phosphate 2-kinase/fructose-2,6-bisphosphatase from Arabidopsis thaliana. Biochem. J. 359: 591–597

Villadsen D, Rung JH, Draborg H & Nielsen TH (2000) Structure and heterologous expression of a gene encoding fructose-6-phosphate,2-kinase/fructose-2,6-bisphosphatase from Arabidopsis thaliana. Biochim. Biophys. Acta 1492: 406–413

Vizcaíno J, Deutsch E & Wang R (2014) ProteomeXchange provides globally coordinated proteomics data submission and dissemination. Nat.32: 223–226

Wang Y, Liu Z, Cheng H, Gao T, Pan Z, Yang Q, Guo A & Xue Y (2014) EKPD: A hierarchical database of eukaryotic protein kinases and protein phosphatases. Nucleic Acids Res. 42: 496–502

Wang ZY & Tobin EM (1998) Constitutive expression of the CIRCADIAN CLOCK ASSOCIATED 1 (CCA1) gene disrupts circadian rhythms and suppresses its own expression. Cell 93: 1207–17

Waterhouse AM, Procter JB, Martin DM a, Clamp M & Barton GJ (2009) Jalview Version 2-A multiple sequence alignment editor and analysis workbench. Bioinformatics 25: 1189–1191

Weig A, Deswarte C & Chrispeels MJ (1997) The Major Intrinsic Protein Family of Arabidopsis Has 23 Members That Form Three Distinct Groups with Functional Aquaporins in Each Group. Plant Physiol. 114: 1347–1357

Wilkinson JQ & Crawford NM (1991) Identification of the Arabidopsis CHL3 gene as the nitrate reductase structural gene NIA2. Plant Cell 3: 461–471

Woods A, Vertommen D, Neumann D, Türk R, Bayliss J, Schlattner U, Wallimannll T, Carling D & Rider MH (2003) Identification of phosphorylation sites in AMP-activated protein kinase (AMPK) for upstream AMPK kinases and study of their roles by site-directed mutagenesis. J. Biol. Chem. 278: 28434–28442

Xu X, Hotta CT, Dodd AN, Love J, Sharrock R, Lee YW, Xie Q, Johnson CH & Webb A a R (2007) Distinct light and clock modulation of cytosolic free Ca2+ oscillations and rhythmic CHLOROPHYLL A/B BINDING PROTEIN2 promoter activity in Arabidopsis. Plant Cell 19: 3474–3490

Xue Y, Ren J, Gao X, Jin C, Wen L & Yao X (2008) GPS 2.0: Prediction of kinase-specific phosphorylation sites in hierarchy 10.1074/mcp.M700574-MCP200. Mol Cell Proteomics: M700574--MCP200

Yang Y, Cheng P, He Q, Wang L & Liu Y (2003) Phosphorylation of FREQUENCY protein by casein kinase II is necessary for the function of the Neurospora circadian clock. Mol. Cell. Biol. 23: 6221–8

Zhang H, Hanley S & Goodman HM (1991) Isolation, characterization, and chromosomal location of a new cab gene from Arabidopsis thaliana. Plant Physiol. 96: 1387–1388

Zhang Y, Feng S, Chen F, Chen H, Wang J, McCall C, Xiong Y & Deng XW (2008) Arabidopsis DDB1-CUL4 ASSOCIATED FACTOR1 forms a nuclear E3 ubiquitin ligase with DDB1 and CUL4 that is involved in multiple plant developmental processes. Plant Cell 20: 1437–55

Acknowledgements

We thank Lisa Imrie, Katalin Kis and Helle K Mogensen for expert technical support. This work was supported by the Wellcome Trust [096995/Z/11/Z] and BBSRC, and EPSRC awards [BB/D019621] and [BB/J009423].

Figure legends

Figure 1: Experimental setup and workflow. a) Plants were grown in 12h light, 12h dark cycles 22 days and then transferred to constant light. In dataset I, rosettes were harvested every 4h from ZT12, in dataset II from ZT24. b) Plants were crushed and protein was extracted, precipitated and digested in-solution. The digest was split into 10µg for global protein analysis (of which 4µg were run) and 490µg for phosphopeptide analysis. Phosphopeptides were enriched using TiO2 spin tips. Global peptides as well as phosphopeptide enriched digests were analysed by LC-MS/MS. Outliers were removed before further bioinformatics analysis.

Figure 2: Venn diagrams showing overlap of quantified (a,c) and rhythmic (WT; b,c) transcripts (Covington *et al*, 2008), proteins and phosphoproteins in dataset I (a,b) and dataset II (c,d).

Figure 3: Heatmap generated by hierarchical clustering of phosphopeptide (top four panels) or global protein (bottom four panels) abundance time courses in dataset I and II (indicated on the right) for WT (a,c) and CCA1-OX (b,d).

Figure 4: Peak time and period distribution of phosphopeptide and protein time courses. a-d: Number of rhythmic (JTK p-value <0.05) phosphopeptides (a,b) or proteins (c,d) peaking at each time point, allowing a period of around 24h (22 to 26) or 12 to 20h. e-f: JTK_CYCLE analysis allowing periods from 12 to 24h on both phosphoproteomics datasets. Number of rhythmic phosphopeptides (JTK < 0.05) for each predicted period is plotted.

Figure 5: Time courses of known direct or suggested SnRK1 targets, phosphopeptides as well as global protein abundance where detected, from both datasets where available. The phosphopeptides of nitrate reductase 1 (a), nitrate reductase 2 (c), are known SnRK1 targets, while the SPS1F (b) and F2KP (d) phosphopeptides shown here have not been reported to be direct targets of SnRK1, but other phosphosite(s) of the proteins are known targets.

Figure 6: Rhythmic kinases. * JTK_CYCLE p-values when allowing shorter periods down to 12h for CCA1-Ox.

Figure 7: Rhythmic or changing phosphatases. * JTK_CYCLE p-values when allowing shorter periods down to 12h for CCA1-Ox. All phosphatases are PP2Cs. At1G09160 (a) was included since ANOVA p-values was significant (WT: 0.031, CCA1-Ox: 0.021).

Figure 8: Examples of proteins with rhythmic abundance. p-values are from JTK_CYCLE analysis.

Figure 9: In vitro GST-F2KP activity assay with WT and Ser276 point mutations. a) F2KP activity at different time points of the reaction. b) Activity calculated from slopes in (a). c) relative quantification of GST-F2KP in eluates probed with rabbit (Rb) anti F2KP and mouse (Ms) anti GST. Original blot is shown below quantification for rabbit anti F2KP. A dilution series of a sample mix was used for quantification, ranging from 0.5 to 1.5 loading equivalent of the samples. Averages of two dilution curves were used. Error bars: SEM. * p-value < 0.05 in t-test. See figure S5 for repeat experiment.

Tables

Table 1: Key numbers for global and phosphoproteomics datasets. a) Numbers of quantified and changing identifications in each dataset, b) shared and added numbers of both datasets. In b) protein IDs of peptides are used since peptide IDs are not comparable between experiments.

a	Dataset I				Dataset II			
	Global Proteomics		Phosphoproteomics		Global Proteomics		Phosphoproteomics	
	WT	CCA1-Ox	WT	CCA1-Ox	WT	CCA1-Ox	WT	CCA1-Ox
Quantifiable identifications before merging	1896 proteins		2287 phosphopeptides		1340 proteins		1664 phosphopeptides	
Quantifiable identifications after merging	n.a.		1498 from 944 proteins		n.a.		1132 from 747 proteins	
Significantly changing (ANOVA p<0.05)	245	147	406	296	68	46	88	83
Adjusted for multiple testing	13	3	56	4	3	2	14	7
Rhythmic by JTK_CYCLE (p<0.05)	171	122	606 from 481 proteins	37 from 32 proteins	45	57	100 from 91 proteins	17 from 17 proteins
Adjusted for multiple testing (q<0.05)	6	0	338	2	6	0	26	0
JTK_CYCLE p<0.05 in both genotypes	17		22		9		3	

b	Global Proteomics		Phosphoproteomics	
	WT	CCA1-Ox	WT	CCA1-Ox
JTK p<0.05 shared	6	3	48	2
all quantified protein Ids shared	137		626	
sum of all quantifiable protein Ids	2501		1065	

Table 2: List of all proteins and phosphopeptides that are rhythmic in WT or CCA1-Ox in both datasets (i.e. shared rhythmic IDs). All p-values are based on JTK_CYCLE analysis. * in some phosphopeptides, the location of phosphorylated residues differs slightly (either shifted by 1-2 residues or one of several phosphates is missing) between datasets, in which case the phosphorylated residues of both datasets are noted (dataset I / dataset II). Bold: phase different of peak is up to 4h. fam. = family, pr. = protein

a) Phosphopeptides, WT

Accession	Description	Peptide ID dataset I	Peptide ID dataset II	Peptide sequence	Phospho residue(s) *	p-value dataset I	p-value dataset II	q-value dataset I	q-value dataset II	Peak dataset I (h)	Peak dataset II (h)
AT4G32340	TPR-like superfam. pr.	15668	12823	SASSLDLNLR	3	9.5E-05	1.9E-09	5.7E-03	2.1E-06	12	32
AT2G33830	Dormancy/auxin associated fam. pr.	6246	2709	TVAAVAGSPGTPTTPGSAR	13 / 11	2.0E-02	2.0E-08	6.5E-02	8.9E-06	12	40
AT4G31700	RPS6A	8624	778	SRLSSAAAKPSVTA	1, 4, 5 / 1, 4, 11	2.0E-06	2.4E-08	4.9E-04	8.9E-06	24	24
AT3G47470	CAB4	715	636	DLSFTSIGSSAK	3	1.3E-06	1.6E-07	4.9E-04	3.0E-05	28	32
AT3G07650	COL9	8182	11184	AGEAYDYDPLTPTRSY	15	3.0E-03	2.4E-07	2.7E-02	3.8E-05	24	40
AT4G31700	RPS6A	8624	1785	SRLSSAAAKPSVTA	1, 4, 5	2.0E-06	2.8E-07	4.9E-04	3.9E-05	24	24
AT5G10360	RPS6B	41, 1736	28	SRLSSAPAKPVAA	4 / 1, 4	7.4E-03	4.8E-07	4.0E-02	5.9E-05	32	24
AT4G31700	RPS6A	8624	21	SRLSSAAAKPSVTA	1, 4, 5 / 1, 4	2.0E-06	9.5E-07	4.9E-04	1.1E-04	24	24
AT5G48250	B-box type zinc finger	11033	16261	SGEAYDYDPMSPTRSY	15 / 16	7.4E-03	1.6E-06	4.0E-02	1.6E-04	24	40
AT1G69870	NRT1.7	7142	8476	ISSPGSILDAEK	3	1.7E-04	3.0E-06	6.8E-03	2.8E-04	24	48
AT5G40890	CLC-A	1783	1852	HRTLSSTPLALVGAK	3, 5	5.1E-05	1.1E-04	4.0E-03	7.3E-03	24	24
AT5G53420	CCT motif family pr.	1950	1997	LGAGLVQSPLDR	8	6.0E-03	1.1E-04	3.6E-02	7.3E-03	28	48
AT5G20670	DUF1677	4202	5127	TSSSGALPGIDGVESR	3 / 4	1.9E-03	1.6E-04	2.3E-02	1.0E-02	28	48
AT1G73980	Phosphoribulokinase / Uridine kinase fam.	10001	8639	LSLDDDTVSSPK	10	1.7E-02	1.9E-04	5.9E-02	1.1E-02	28	24
AT1G78020	DUF581	10297, 1700	3249, 1093	LLSMVTPR	3	1.3E-05	2.1E-04	1.5E-03	1.2E-02	24	24
AT1G78020	DUF581	2081, 5542, 5542	2113, 737, 2081	RHSGDFSDAGHFLR	3	2.4E-02	1.5E-03	7.4E-02	6.2E-02	24	24
AT1G11310	MLO2	1496	3909	SVENYPSSPSPR	7 / 8, 10	2.3E-04	1.9E-03	7.7E-03	6.9E-02	32	24
AT4G31700	RPS6A	2489	3985	LSSAAAKPSVTA	9	1.5E-03	3.6E-03	2.1E-02	1.2E-01	32	48
AT2G32240	unknown	5883	7383	DIDLSFSSPTKR	8	1.1E-02	4.0E-03	4.9E-02	1.3E-01	24	48
AT3G13290	VCR	4140	6826	TLSYPTPPLNPQSPR	13	3.0E-03	5.4E-03	2.7E-02	1.6E-01	28	48
AT4G35100	PIP3A	140	214	ALGSFRSNATN	4, 7	1.1E-02	8.0E-03	4.9E-02	1.9E-01	28	24
AT5G38640	NagB/RpiA/CoA transferase-like superfam. pr.	4683	1690	DFPDGSTTASPGR	10	6.0E-03	8.8E-03	3.6E-02	2.0E-01	32	24
AT1G37130	NIA2	4382	2045, 2045	VHDDDEDVSSEDENETHNSNAVYYK	9, 10	9.0E-04	8.8E-03	1.7E-02	2.0E-01	28	28
AT3G13530	MAPKKK7	3515	6312	SKLPLVGVSSFR	10	3.0E-03	8.8E-03	2.7E-02	2.0E-01	28	40
AT1G35580	CINV1	903	1066	SVLDTPLSSAR	5, 8	1.7E-02	9.7E-03	5.9E-02	2.1E-01	24	24
AT1G74780	Major Facilitator Superfam. pr.	6279	4702, 5728	TVPHDYSPLISSPK	12	3.0E-03	9.7E-03	2.7E-02	2.1E-01	28	48
AT3G27700	zinc finger fam. pr.	9563	9073	LDTASDSGAAIASPK	13	4.8E-03	1.1E-02	3.4E-02	2.2E-01	28	48
AT5G65010	ASN2	4975	4842	AGSDLVDPLPK	3	6.9E-04	1.3E-02	1.6E-02	2.4E-01	28	24
AT4G31160	DCAF1, DDB1-CUL4 associated factor 1	8754	7154, 8583	VHEGAPDTEVLLASPR	14	3.5E-02	1.3E-02	9.3E-02	2.4E-01	28	48
AT4G13510	AMT1;1	214	110	SPSPSGANTTPTPV	1	3.5E-02	1.4E-02	9.3E-02	2.5E-01	32	48
AT5G23660	SWEET12	14806	17187	LGTLTSPEPVAITVVR	6	9.1E-03	1.8E-02	4.3E-02	3.0E-01	24	40
AT3G26730	RING/U-box superfam. pr.	5794	6017	NQTQSLSPPDVSR	7	1.3E-04	2.2E-02	6.2E-03	3.5E-01	24	24
AT4G20910	HEN1	15648	13859, 13859	SSSPNVFAAPPILQK	3 / 2, 3	9.5E-05	2.6E-02	5.7E-03	3.7E-01	28	24
AT2G07360	SH3 domain-containing pr.	2769, 5085	9464, 8286	YQSTYEGYGSPIREEPPPPYSYSEPQSR	10	1.1E-02	2.6E-02	4.9E-02	3.7E-01	24	36
AT4G26130	unknown pr.	5416, 7652, 1518	7456	TTSIGDGGEEGVDDKASNFINK(FK)	3	1.4E-02	2.6E-02	5.3E-02	3.7E-01	24	40
AT1G44800	nodulin MtN21	7377	34568	SQELPITNVVK	1	4.4E-06	2.6E-02	6.5E-04	3.7E-01	28	52
AT2G46920	POL	7848	11608	SNFSAPLSFR	8	1.9E-03	3.1E-02	2.3E-02	4.1E-01	28	40
AT2G42600	PPC2	1672, 57	62, 40, 4070	MASIDAQLR	3	7.4E-03	4.0E-02	4.0E-02	4.7E-01	32	24
AT3G60240	EIF4G	1585	1579	QVLQGPSATVNSPR	12	3.8E-03	4.3E-02	3.0E-02	4.9E-01	28	48
AT1G70770	DUF2359	514	169, 800	MTAIDSDDDGVVR	6	7.4E-03	4.3E-02	4.0E-02	4.9E-01	24	48
AT5G40890	CLC-A	749	406	TLSSTPLALVGAK	3	1.3E-04	4.3E-02	6.2E-03	4.9E-01	28	48
AT4G12770	Chaperone DnaJ-domain superfam. pr.	238, 238	318	FENVFSSISSSPTK	11	6.0E-03	4.7E-02	3.6E-02	5.2E-01	28	48

Table 2 *continued*

b) Phosphopeptides, CCA1-Ox

Accession	Description	Peptide ID dataset I	Peptide ID dataset II	Peptide sequence	Phospho residue(s) *	p-value dataset I	p-value dataset II	q-value dataset I	q-value dataset II	Peak dataset I (h)	Peak dataset II (h)
AT2G33830	Dormancy/auxin associated fam. pr.	1348, 43281	2709	TVAAVAGSPGTPT TPGSAR	11	0.023	0.0069	1	1	12	24
AT1G51805	Leucine-rich repeat protein kinase fam. pr.	2617	2514, 1136	VEGTLPSYMQASD GRSPR	16	0.019	0.021	1	1	24	24

c) Phosphoproteomics, CCA1-Ox, allowing periods 12 to 20h

Accession	Description	Peptide ID dataset I	Peptide ID dataset II	Peptide sequence	Phospho residue(s) *	p-value dataset I	p-value dataset II	q-value dataset I	q-value dataset II	Peak dataset I (h)	Peak dataset II (h)
AT1G77760	NIA1	4776	1968	SVSSPFMNTASK	3	0.013	0.00067	0.42	0.25	24	48
AT2G45820	Remorin fam. pr.	1234, 5319	698, 2343	ALAVVEKPIEEHTP K	13	0.019	0.0045	0.42	0.68	24	24

d) Global proteomics, WT

Accession	Description	p-value dataset I	p-value dataset II	q-value dataset I	q-value dataset II	Peak dataset I (h)	Peak dataset II (h)
AT4G39800	MI-1-P SYNTHASE	6E-06	9E-12	0.00588435	5.8E-09	28	24
AT4G17090	BAM3	0.0056	5E-05	0.225379284	0.01543	20	44
AT5G13630	GUN5	0.0301	1E-04	0.427829153	0.02763	32	52
AT1G78570	RHM1	0.0005	6E-04	0.070946877	0.08717	28	48
AT1G15820	LHCB6	0.044	0.023	0.516391687	0.92673	12	36
AT4G27440	PORB	0.0003	0.03	0.06492429	1	12	36

e) Global proteomics, CCA1-Ox

Accession	Description	p-value dataset I	p-value dataset II	q-value dataset I	q-value dataset II	Peak dataset I (h)	Peak dataset II (h)
AT3G47070	unknown	0.0342	0.012	0.634454201	0.90965	20	40
AT3G49190	O-acyltransferase fam. pr.	0.0016	0.022	0.24526271	0.91655	32	44
AT4G39800	MI-1-P SYNTHASE	0.0004	0.034	0.175519785	0.98762	24	24

Table 3: Summary of GO analysis. Listed are terms that occur either in both datasets (c,d) or both genotypes (a,c) in the phosphoproteomics (a,b) and global proteomics (c,d) analyses. ZTs at which GO terms are enriched are indicated. In bold: Shared terms where peaks are maximum 4h apart (i.e. 4h or 20h or 28h). Full GO lists are in supplementary data S3.

a) Common between genotypes, phosphoproteomics:

groups	GO ID	description	ZT WT	ZT CCA1-Ox
dataset I	**GO:0008168**	**methyltransferase activity**	**28**	**24**
dataset I including CCA1-Ox shorter periods	**GO:0055074**	**calcium ion homeostasis**	**24**	**24**
	GO:0006012	**galactose metabolic process**	**24**	**24**
	GO:0042803	**protein homodimerization activity**	**28**	**24**
	GO:0000287	**magnesium ion binding**	**28**	**24**
	GO:0008553	**hydrogen-exporting ATPase activity, phosphorylative mechanism**	**28**	**24**
	GO:0015976	**carbon utilization**	**28**	**24**
	GO:0015991	**ATP hydrolysis coupled proton transport**	**28**	**24**
dataset II	none			
dataset II including CCA1-Ox shorter periods	GO:0003700	transcription factor activity, sequence-specific DNA binding	40	24 or 48
	GO:0006355	regulation of transcription, DNA-templated	40	24 or 48

b) Common between datasets, phosphoproteomics

groups	term	description	ZT dataset I	ZT dataset II
WT	GO:0048825	cotyledon development	32	48
CCA1-Ox	none			

c) Common between genotypes, global proteomics:

groups	term	description	ZT WT	ZT CCA1-Ox
dataset I	**GO:0010200**	**response to chitin**	**12**	**32**
	GO:0016616, GO:0016628	**oxidoreductase activity, acting on the CH-CH group of donors, NAD or NADP as acceptor**	**32**	**12**
dataset II	none			

d) Common in datasets, global proteomics:

groups	term	description	ZT dataset I	ZT dataset II
WT	**GO:0016168**	**chlorophyll binding**	**12**	**36**
	GO:0009902	chloroplast relocation	12	44
	GO:0035304	**regulation of protein dephosphorylation**	**12**	**36**
	GO:0010218	response to far red light	12	44
	GO:0010114	response to red light	12	44
	GO:0009637	response to blue light	12	44
	GO:0019344	**cysteine biosynthetic process**	**12**	**36**
	GO:0010027	thylakoid membrane organization	12	44
	GO:0019684	**photosynthesis, light reaction**	**12**	**36**
	GO:0006098	pentose-phosphate shunt	12	44
	GO:0009744	**response to sucrose**	**12**	**32**
	GO:0016616, GO:0016628	**oxidoreductase activity, acting on the CH-CH group of donors, NAD or NADP as acceptor**	**32**	**36**
CCA1-Ox	**GO:0052541**	**plant-type cell wall cellulose metabolic process**	**20**	**44**
	GO:0052546	**cell wall pectin metabolic process**	**20**	**44**

Table 4: Summary of GPS3 kinase prediction followed by Fisher's Exact test. Fisher's exact test p-values for enrichment of each kinase group are shown. a) dataset I, b) dataset II. Foreground groups were chosen with JTK_CYCLE p-values <0.05 and peaks or troughs at indicated ZTs. For same analysis using ANOVA p-values see table S1.

a

	WT, 22 to 26h period				CCA1-Ox, 22 to 26h period			CCA1-Ox, 12 to 20h period
	peak		trough	all p<0.05	peak	trough	all p<0.05	peak
time point	24h	28h	12h		24h	12h		24h
AGC					0.043			
AGC/NDR		0.0072						
Atypical/TAF1	6.50E-06		2.50E-06					
CAMK		0.0012		0.0040		0.00063	0.0090	0.024
CAMK/DAPK								0.029
CMGC/CK2	0.0012		4.70E-06					
CMGC/MAPK				0.027				
Other / ULK			0.040			0.0030	0.0066	
Other/WNK								0.044

b

	WT, 22 to 26h period			CCA1-Ox, 22 to 26h period		CCA1-Ox, 12 to 20h period
	peak		all p<0.05	peak	all p<0.05	peak
time point	24h	48h		24h		24h
AGC	1.4E-06					
AGC/PDK1	0.0049					
CAMK	0.00024		0.0049			0.048
CAMK-L						0.0035
CAMK-Unique	0.057					
CMGC	0.0061			0.040		
CMGC/GSK	0.0078					
CMGC/MAPK		0.040				
Other/PEK				0.028	0.047	
STE/STE7	0.037					

Figures

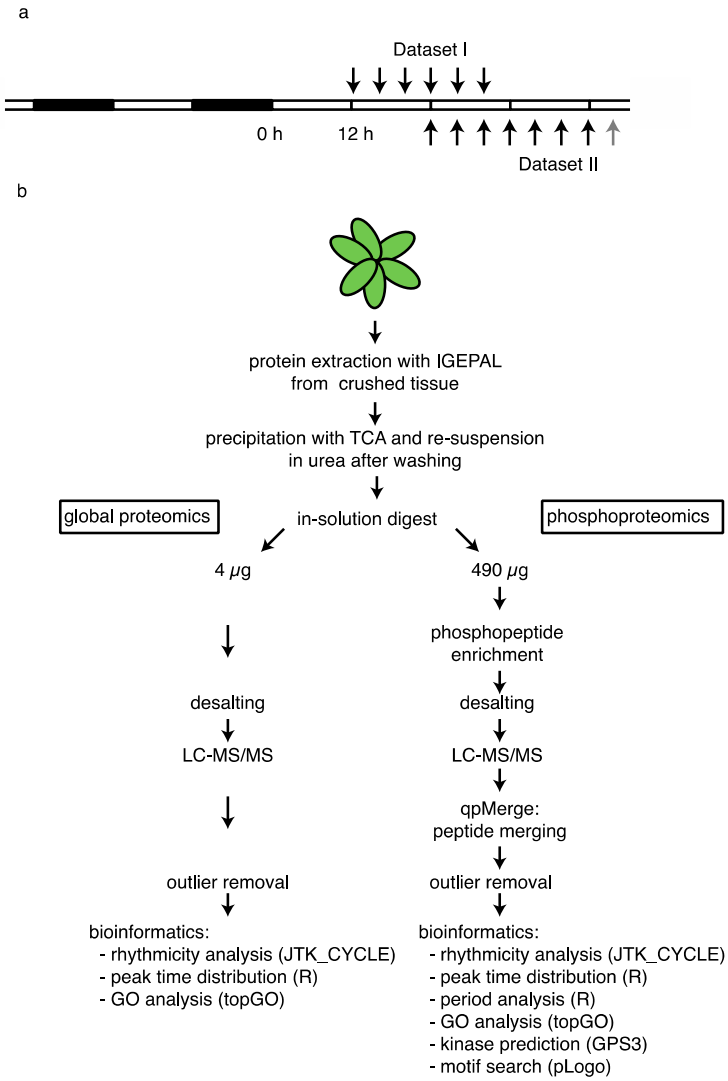

Figure 1: Experimental setup and workflow. a) Plants were grown in 12h light, 12h dark cycles 22 days and then transferred to constant light. In dataset I, rosettes were harvested every 4h from ZT12, in dataset II from ZT24. b) Plants were crushed and protein was extracted, precipitated and digested in-solution. The digest was split into 10µg for global protein analysis (of which 4µg were run) and 490µg for phosphopeptide analysis. Phosphopeptides were enriched using TiO_2 spin tips. Global peptides as well as phosphopeptide enriched digests were analysed by LC-MS/MS. Outliers were removed before further bioinformatics analysis.

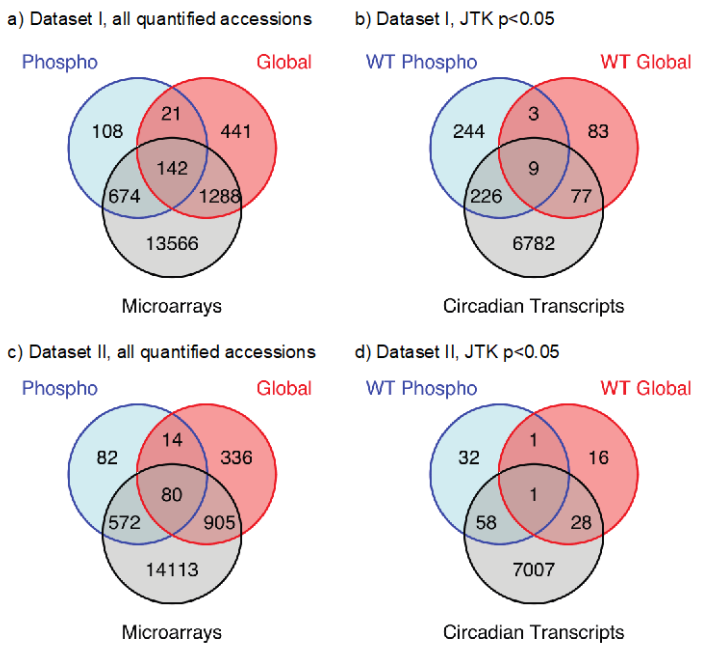

Figure 2: Venn diagrams showing overlap of quantified (a,c) and rhythmic (WT; b,c) transcripts (Covington *et al*, 2008)**, proteins and phosphoproteins in dataset I (a,b) and dataset II (c,d).**

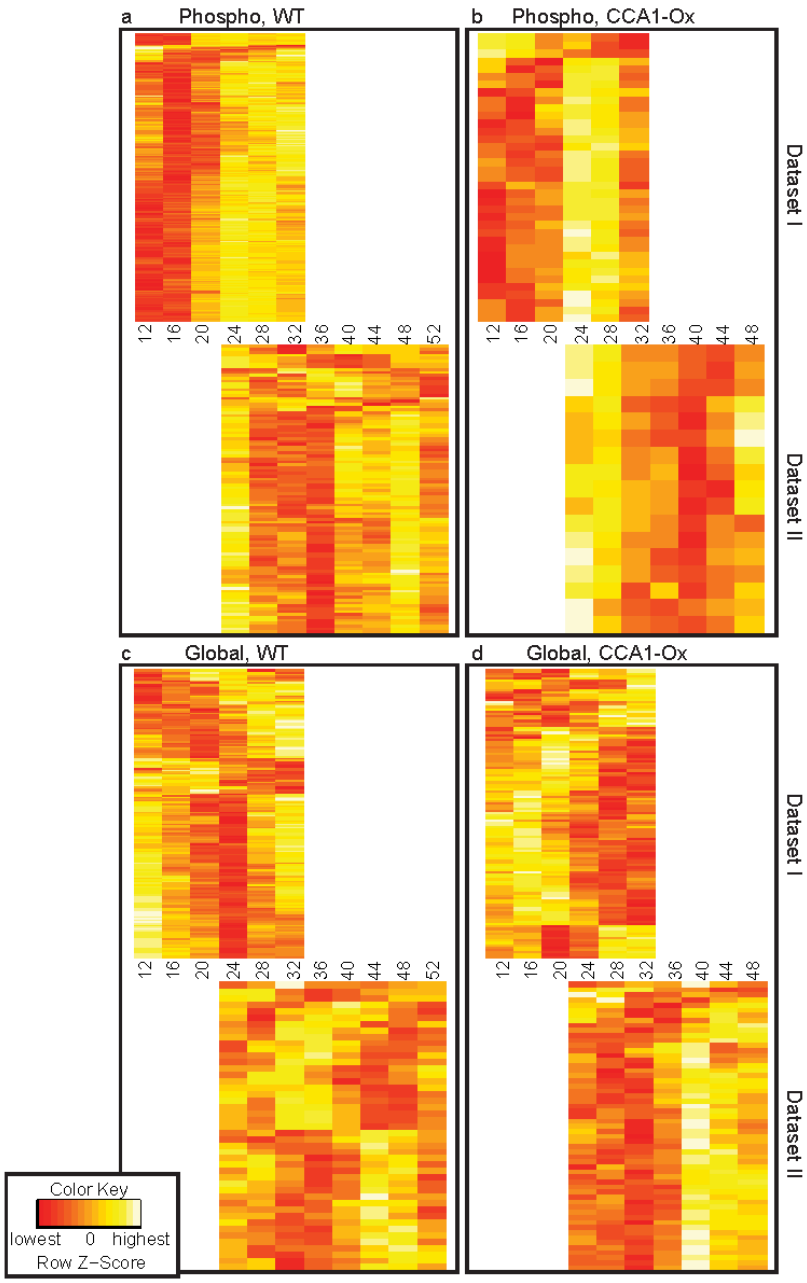

Figure 3: Heatmap generated by hierarchical clustering of phosphopeptide (top four panels) or global protein (bottom four panels) abundance time courses in dataset I and II (indicated on the right) for WT (a,c) and CCA1-OX (b,d).

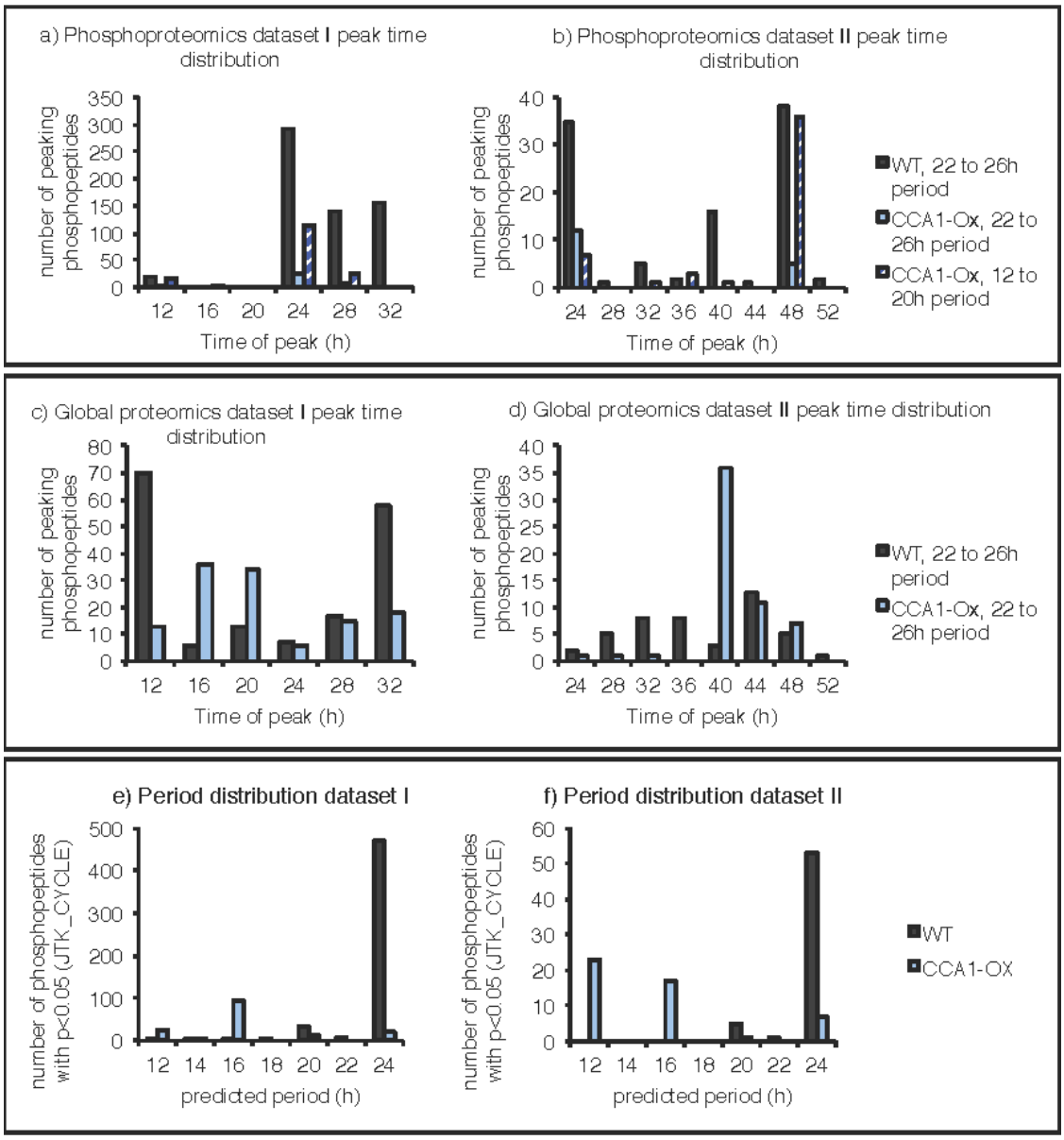

Figure 4: Peak time and period distribution of phosphopeptide and protein time courses. a-d: Number of rhythmic (JTK p-value <0.05) phosphopeptides (a,b) or proteins (c,d) peaking at each time point, allowing a period of around 24h (22 to 26) or 12 to 20h. e-f: JTK_CYCLE analysis allowing periods from 12 to 24h on both phosphoproteomics datasets. Number of rhythmic phosphopeptides (JTK < 0.05) for each predicted period is plotted.

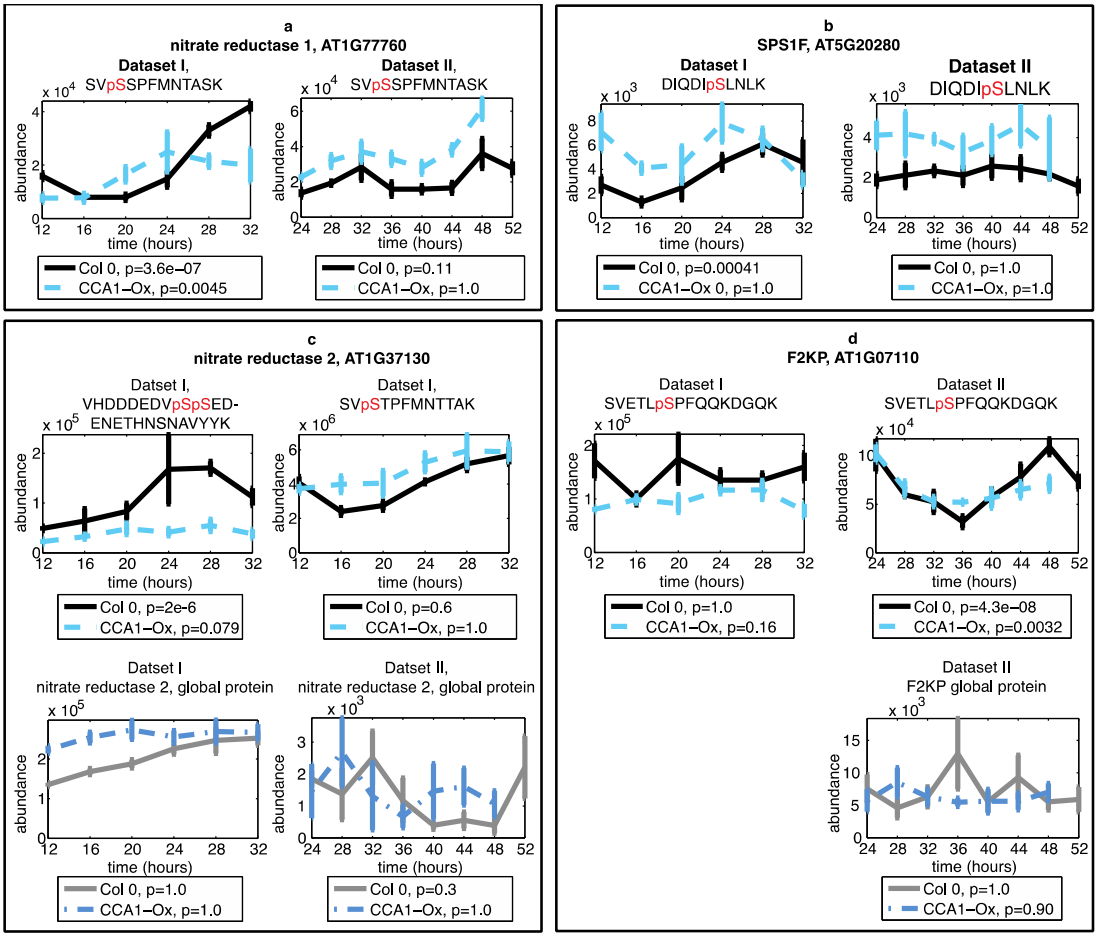

Figure 5: Time courses of known direct or suggested SnRK1 targets, phosphopeptides as well as global protein abundance where detected, from both datasets where available. The phosphopeptides of nitrate reductase 1 (a), nitrate reductase 2 (c), are known SnRK1 targets, while the SPS1F (b) and F2KP (d) phosphopeptides shown here have not been reported to be direct targets of SnRK1, but other phosphosite(s) of the proteins are known targets.

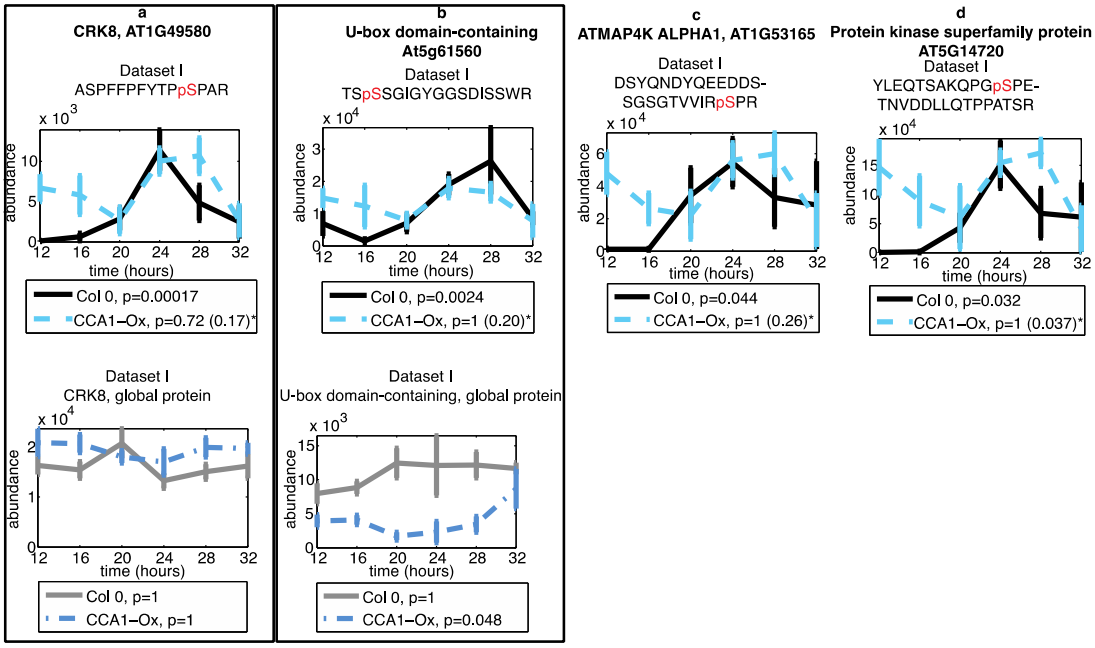

Figure 6: Rhythmic kinases. * JTK_CYCLE p-values when allowing shorter periods down to 12h for CCA1-Ox.

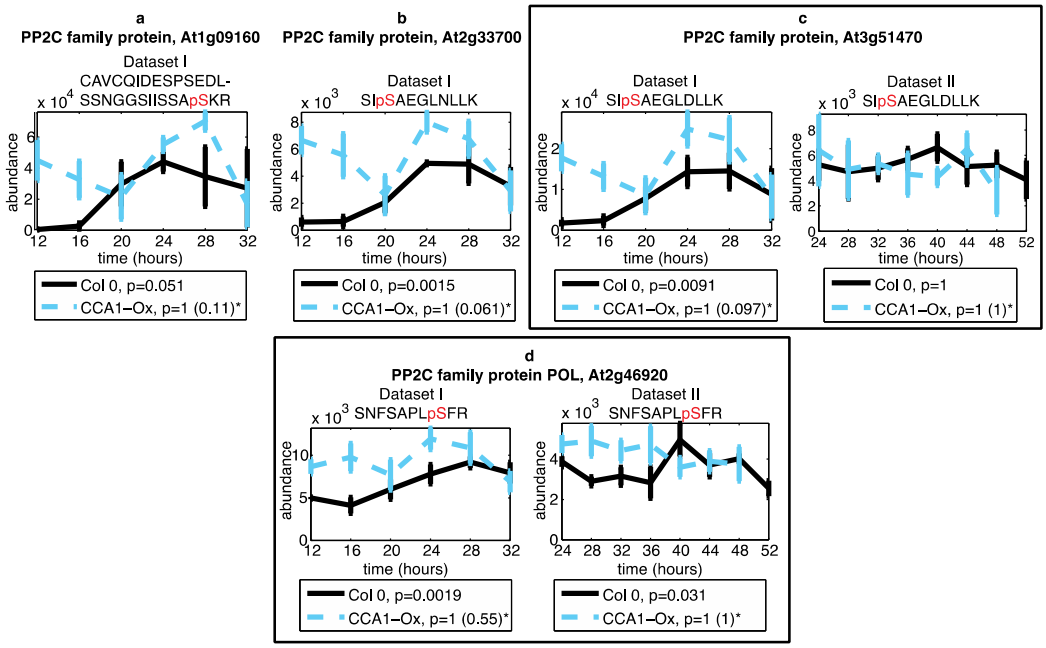

Figure 7: Rhythmic or changing phosphatases. * JTK_CYCLE p-values when allowing shorter periods down to 12h for CCA1-Ox. All phosphatases are PP2Cs. At1G09160 (a) was included since ANOVA p-values was significant (WT: 0.031, CCA1-Ox: 0.021).

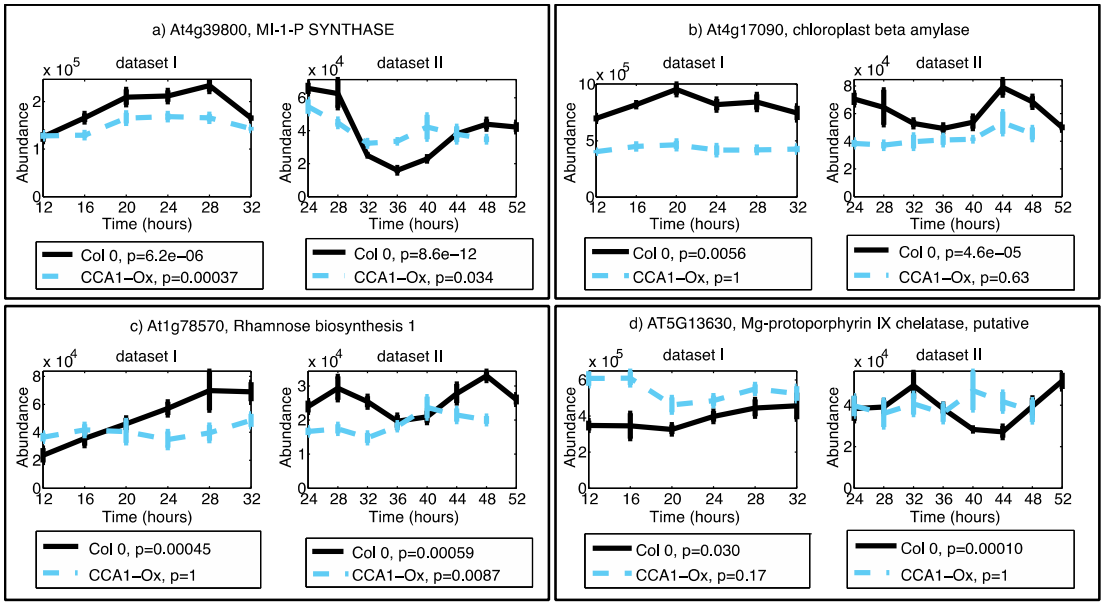

Figure 8: Examples of proteins with rhythmic abundance. p-values are from JTK_CYCLE analysis.

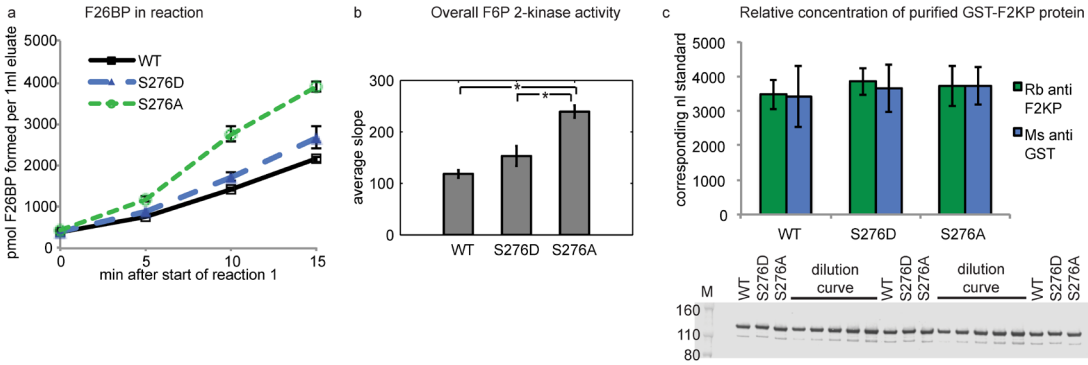

Figure 9: In vitro GST-F2KP activity assay with WT and Ser276 point mutations. a) F2KP activity at different time points of the reaction. b) Activity calculated from slopes in (a). c) relative quantification of GST-F2KP in eluates probed with rabbit (Rb) anti F2KP and mouse (Ms) anti GST. Original blot is shown below quantification for rabbit anti F2KP. A dilution series of a sample mix was used for quantification, ranging from 0.5 to 1.5 loading equivalent of the samples. Averages of two dilution curves were used. Error bars: SEM. * p-value < 0.05 in t-test. See figure S5 for repeat experiment.

Supplementary figures

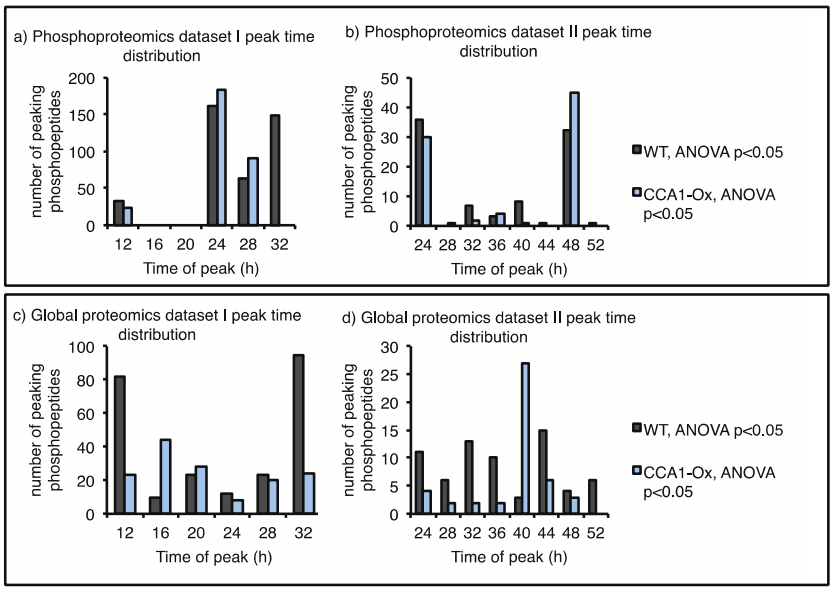

Figure S 1: Peak time distribution of changing (ANOVA p<0.05) phosphopeptides (a.b) and proteins (c,d) in datasets I (a,c) and II (b,d).

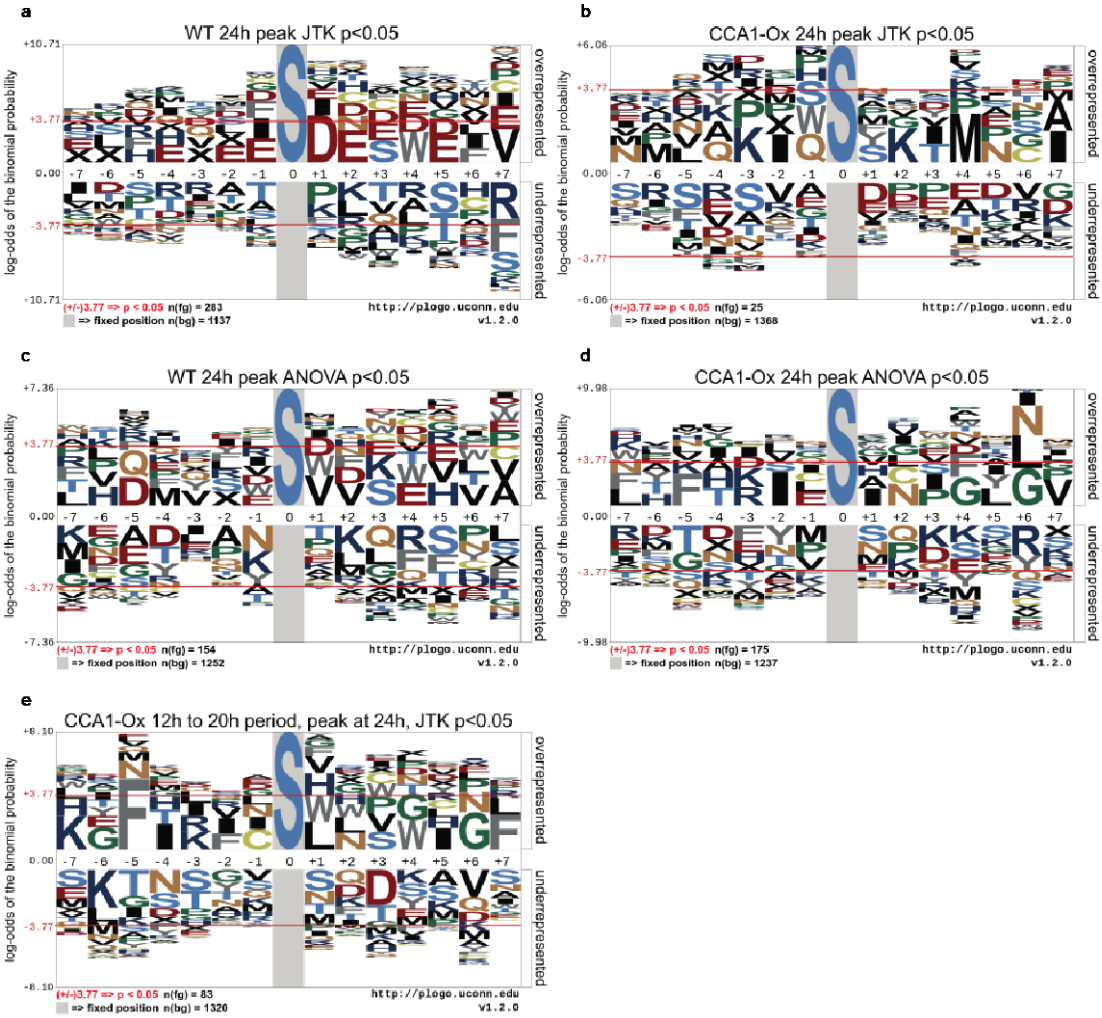

Figure S 2: pLogos generated for phosphoproteomics dataset I. (a-b) using peptides as foreground with JTK_CYCLE p<0.05 (allowed periods 22h to 26h) and peaking at 24h for (a) WT and (b) CCA-1Ox, (c-d) using peptides as foreground with ANOVA p<0.05 and peaking at 24h for WT (c) and CCA1-Ox (d). (e) CCA1-Ox JTK_CYCLE p<0.05 when allowing periods 12h to 20h, and peaking at 24h.

Figure S 3: pLogos generated for phosphoproteomics dataset II. (a,c) For the WT, phosphopeptides with JTK_CYCLE p-value <0.05 were chosen that peak at either 24h (a) or 48h (c). (e,g) Like (a,c) but using ANOVA p-values <0.05 instead of JTK_CYCLE (b,d) For CCA1-Ox phosphopeptides with JTK_CYCLE p-value <0.05 and peaking at 24h or 48h (identical to all significant phosphopeptides for (b)) and a period of 22 to 26h (b) or a period of 12h to 16h (d). (f,h) same as (e,g) for CCA1-Ox.

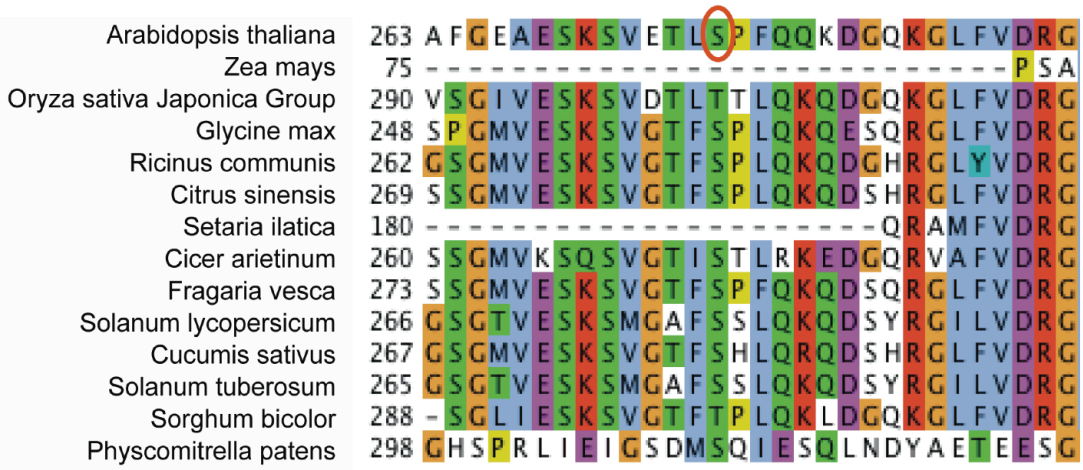

Figure S 4: Alignment of sequence area surrounding S276 in a selection of plant species. S276 is highlighted with a red circle in the Arabidopsis thaliana sequence. Amino acid sequences of F2KP from several plant species were aligned using the Jalview software (Waterhouse *et al*, 2009)**. The *Arabidopsis thaliana* sequence was obtained from tair (www.arabidopsis.org, accession AT1G07110), the other sequences from ncbi (http://www.ncbi.nlm.nih.gov). Accessions on ncbi were: XP_002440665 (*Sorghum bicolor*), XP_006350851 (*Solanum tuberosum*), XP_004166327 (*Cucumis sativus*), XP_004242511 (Solanum lycopersicum), XP_004294306 (*Fragaria vesca*), XP_004490623 (*Cicer arietinum*), XP_- 004984866 (Setaria italica), XP_006488693 (Citrus sinensis), XP_002514503 (*Ricinus communis*), XP_003552945 (*Glycine max*), NP_001054740 (*Oryza sativa* Japonica group) and NP_00114823 (*Zea mays*).**

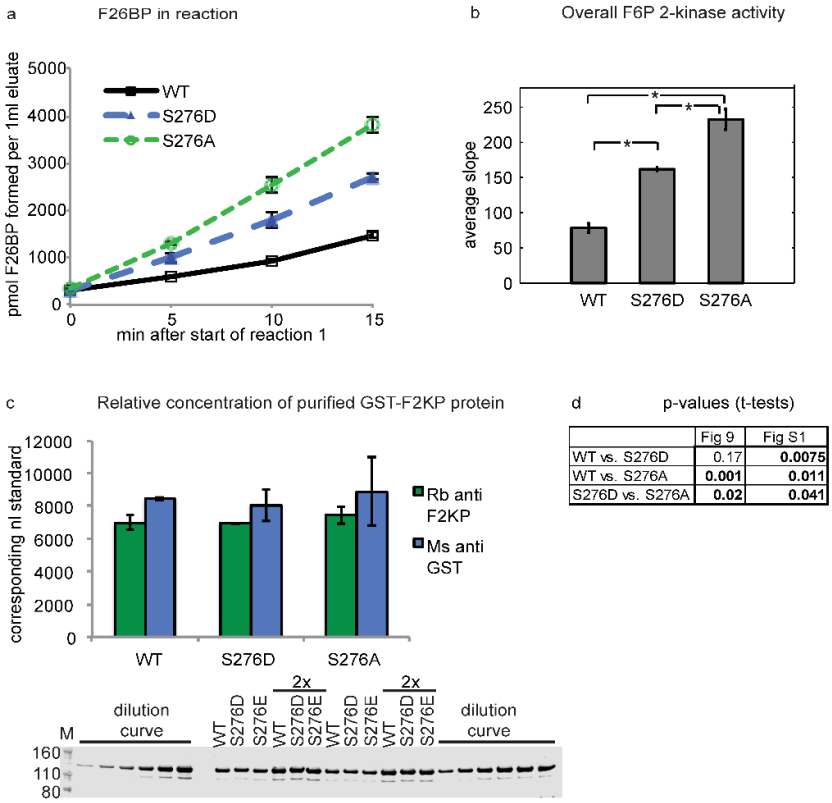

	Fig 9	Fig S1
WT vs. S276D	0.17	**0.0075**
WT vs. S276A	**0.001**	**0.011**
S276D vs. S276A	**0.02**	**0.041**

Figure S 5: In vitro GST-F2KP activity assay with WT and Ser276 point mutations. Repeat experiment of Figure 9. a) F2KP activity at different time points of the reaction. b) Activity calculated from slopes in (a). c) relative quantification of GST-F2KP in eluates probed with rabbit (Rb) anti F2KP and mouse (Ms) anti GST. Original blot is shown below quantification for rabbit anti F2K. A dilution series of a sample mix was used for quantification, ranging from 0.5 to 1.5 loading equivalent of the samples. Averages of two dilution curves were used. (d) p-values of F2KP activity in figure 9 and this figure. Error bars: SEM. * p-value < 0.05 in two-sided t-test.

Supplementary tables

Table S 1: ***GPS3 kinase prediction, using ANOVA p-values.*** **ANOVA analysis on each phosphosite time course was carried out on the data after outlier exclusion, treating 0 values as missing values. GPS3 predictions from Phosphopeptides with ANOVA p-values less than 0.05 were used as foreground for testing enrichment of kinases predictions in all significantly changing phosphopeptides, while phosphopeptides with p<0.05 and a given peak time were used to analyse for enrichment at specific times of the day (24 or 48h). In the case of several predicted kinases within a family of kinases for the same phosphosite, only the one with the highest difference of score and cutoff was considered. Predictions for each kinase were counted in the foreground as well as the background and a Fisher's exact test was used to test for significant enrichment. Fisher's test p-values are shown in the table. Only p-values <0.05 are shown and only for over-representation of predictions rather than under-representation.**

	Phosphoproteomics dataset I								Phosphoproteomics dataset II				
	WT				CCA1-Ox				WT		CCA1-Ox		
		peaks				peaks				peaks		peaks	
EKPD kinase group	all p<0.05	12h	24h	28h	all p<0.05	23h	24h	28h	all p<0.05	24h	all p<0.05	24h	48h
AGC	0.0015												
AGC/PDK1	0.0000011							0.026					
Atypical/TAF1								0.0038	0.022		0.0044		
CAMK	0.00000072			0.022			0.034		0.0013	0.001		0.022	
CAMK/CAMK-Unique	0.000075								0.014	0.0071			
CAMK/CAMK1									0.036				
CAMK/CAMKL	0.0036												
CMGC	0.000026							0.048		0.035			
CMGC/CK2								0.0048	0.011		0.033		
CMGC/DYRK	0.00619												
CMGC/GSK	0.00024												
CMGC/MAPK	0.00010	0.010											
CMGC/CDK	0.000026												
CK1/CK1	0.012												
STE/STE11	0.015		0.020								0.029		0.039
STE/STE7	0.003												
TK					0.045								
TKL/IRAK											0.0037		0.0083
Other/Haspin						0.00027							
Other/WNK							0.040						
Other/TTK					0.045			0.026					

Table S 2: List of known and some suggested SnRK1 targets as well as JTK_CYCLE and ANOVA p-values on both experiments and genotypes, phosphopeptides found in this analysis as well as published literature.

Accession and name	reference	published peptide	peptide in analysis	JTK_pvalue	ANOVA pvalue
AT1G07110 F2KP	Cho *et al*, 2016	SVETL**pS**PFQQK	SVETL**pS**PFQQK DGQK	dataset 1: WT: 1.0 CCA1-Ox: 0.16 dataset2: WT: **4.3x10^{-8}** CCA1-Ox: **0.0032**	dataset1: WT: 0.48 CCA1-Ox: 0.096 dataset2: WT: **1.2x10^{-5}** CCA1-Ox: **0.048***
AT1G77760, nitrate reductase 1	Sugden *et al*, 1999	spinach: TLKRTA**pS**TPFM	SV**pS**SPFMNTASK	dataset I: WT: **3.6*10^{-7}** CCA1-Ox: **0.0045** datasetII, JTK: WT: 0.11 CCA1-Ox: 1	dataset I: WT: **2.95*10^{-7}** CCA1-Ox: 0.064 dataset II: WT: **0.042** CCA1-Ox: **8.3x10^{-5}**
(published experiment in spinach) nitrate reductase 2	Sugden *et al*, 1999	spinach: TLKRTA**pS**TPFM	SV**pS**TPFMNTTAK	dataset I: WT: **2x10^{-6}** CCA1-Ox: 0.079 dataset II: WT: 0.60 CCA1-Ox: 1.0	dataset I: WT: **1.1x10^{-5}** CCA1-Ox: **0.048** dataset II: WT: 0.075 CCA1-Ox: 0.084
SPS1F At5g20280	Sugden *et al*, 1999	spinach: RMRRIS**pS**VEMM	DIQDI**pS**LNLK	dataset I: WT: **0.00041** CCA1-Ox: 1.0 dataset II: WT: 1.0 CCA1-Ox: 1.0	dataset I: WT: **0.0088** CCA1-Ox: 0.079 dataset II: WT: 0.87 CCA1-Ox: 0.83

Table S 3: List of primers for point mutagenesis and subcloning of F2KP

Primer name	Mutation	Sequence
AspF	S276D	ACCATCTTTCTGCTGAAACGGATCGAGTGTCTCCACAGACTTTGA
AspR	S276D	TCAAAGTCTGTGGAGACACTCGATCCGTTTCAGCAGAAAGATGGT
AlaF	S276A	CATCTTTCTGCTGAAACGGAGCGAGTGTCTCCACAGACTTT
AlaR	S276A	AAAGTCTGTGGAGACACTCGCTCCGTTTCAGCAGAAAGATG
F2KP-F	none	GAGCTTAAGATGGGGTCAGGTGCATCGAAGAATAC
F2KP-R	none	AGCTCTAGATCAGTCCATGAGTTTGTAGCGTTTCTCTTGC

Table S 4: detection of SnRK1 target sequences in various foregrounds and backgrounds and resukts of Fisher's Exact test p-value. One sub-table for each dataset. 'Hits' are peptides which fulfill the SnRK1 target pattern [M, L, V, I, F] X X X X [S, T] X X X [M, L, V, I, F]

Dataset I

Genotype	Allowed periods	peak time point	Fisher pvalue	% in foreground	% in background	number of hits foreground	total foreground	number of hits background	total background
WT	22 to 26h	12	0.20	14.29	7.25	3	21	113	1558
WT	22 to 26h	24	0.72	6.75	7.54	22	326	97	1286
WT	22 to 26h	28	0.74	8.22	7.46	12	146	108	1448
WT	22 to 26h	32	0.21	4.73	7.57	8	169	108	1426
WT	22 to 26h	any	0.44	6.65	7.79	43	647	76	976
CCA1-Ox	22 to 26h	24	0.45	10.71	7.29	3	28	113	1551
CCA1-Ox	22 to 26h	any	1.00	7.50	7.32	3	40	113	1543
CCA1-Ox	12 to 20h	24	0.55	9.18	7.37	9	98	110	1492

Dataset II

Genotype	Allowed periods	peak time point	Fisher pvalue	% in foreground	% in background	number of hits foreground	total foreground	number of hits background	total background
WT	22 to 26h	24	0.04	0.00	8.57	0	42	101	1178
WT	22 to 26h	48	0.77	5.00	8.43	2	40	99	1175
WT	22 to 26h	any	0.59	6.25	8.45	7	112	94	1112
CCA1-Ox	22 to 26h	24	**0.00047**	**58.33**	**8.33**	**7**	**12**	**100**	**1200**
CCA1-Ox	22 to 26h	any	1.00	5.88	8.37	1	17	100	1195
CCA1-Ox	12 to 20h	24 or 48	0.21	14.29	8.15	5	35	96	1178

Supplementary methods

Outlier analysis

Two measures were used to identify statistical outliers on arcsinh transformed data: Pearson correlation analysis and PCA. Both were calculated in an R script included in Data S4. PCA was calculated within each time course and genotye. The Pearson correlation coefficient of peptide or protein abundance values of each replicate with the time point median was determined. For phosphopeptide data, all replicates in which the Pearson correlation coefficient was < 0.8 were regarded as outliers. The PCA analysis and plots of the difference to the sample median served to validate the exclusion of replicates. In the global data analysis of datase II, these measures revealed a machine drift and we regarded it as necessary to remove each first-run replicate of each time point.

These criteria resulted in removal of the following replicates as outliers:

Phospho I dataset – WT: 12D, 16B, 24A, 28B, 32A, 32B; CCA1.OX: 20D, 24E, 28C, 32C

Global I dataset: no outliers

Phospho II dataset – WT: 24E, 28D, 28F, 32A, 32D, 32H, 40B, 40F, 44D, 48F, 52F; CCA1-OX: 28E, 32D, 36E, 40D, 48E

Global II dataset – WT: 24A; 28A, 28B, 28F, 32A, 36A, 40A, 44A, 48F, 52A; CCA1-OX: 24A, 28A, 32A, 36A, 40A, 44A, 48A, 52A

All plots of PCA, Pearson correlation coefficient and boxplots of median of replicate minus time point mean are included in DataS4.

pLogo generation

The online tool pLogo was used to visualize enrichment of amino acids at the 14 positions surrounding phosphorylated serine or threonine residues (O'Shea *et al*, 2013). A python script was used to generate lists of phosphosites for foreground and background with 7 amino acids on either side of the phosphorylated position.

As foreground, rhythmic (JTK_CYCLE $p<0.05$) or significantly changing (ANOVA $p<0.05$) were used, either the group or all significant phosphopeptides or the subgroup phosphopeptides that peak at 24h or 48h or both. The background consisted of all phosphopeptides detected in the respective experiment (dataset I or II) without the foreground.

SnRK1 target pattern prediction

SnRK1 target patterns were specifically searched using a python script and the motif X [M, L, V, I, F] X X X X [S, T] X X X [M, L, V, I, F] (Broeckx *et al*, 2016), X being any amino acid. Alternatively, the requirement for a basic amino acid was included at either position -3 or -4 with respect to the phosphorylated serine or threonine.

We used the same 15 amino acid sequences frames as for the pLogo generation to detect the SnRK1 target pattern, i.e. searched for phosphorylation sites with hydrophobic residues at the -5 and +4 positions using a python script. We then performed Fisher's exact tests using R to determine whether SnRK1 patterns are significantly enriched in any of the groups tested. We only tested groups with JTK_CYCLE p-value < 0.05 where the foreground consisted of at least 10 peptide, together with peak time point requirements and different allowed period lengths. The results are shown in Table S 4.

Supplementary files:

Data S1: Peptide measurements progenesis export

Data S2: Protein measurements progenesis export

Data S3: All phosphopeptide and global protein data tables without outliers, including statistics

Data S4: Outlier analysis files, phospho II WT as example:

- input file: outlier_input.csv
- outlier analysis script: outlier.R
- PCA output file: outlier_PCA.pdf
- Correlation analysis output file: outlier_boxplot.pdf
- File with all PCA and correlation analysis output plots: OutlierFigures.pdf

Data S5: JTK_CYCLE analysis files, phospho II WT as example:

- JTK_CYCLE resource file (published but needed for running the analysis): JTK_CYCLE.R
- script used to run JTK_CYCLE, adapted: run_JTK.R
- metadata file for JTK_CYCLE analysis: metadata.csv
- example input data for JTK_CYCLE analysis: input_data.csv
- output data for this example: JTK_output.xlsx

Data S6: Gene ontology analysis using the topGO R package, Phospho I WT as example

- script to run topGO: topGO_analysis.R
- example input file: topGO_input.csv
- gene associations input file from tair: gene_association.csv.csv
- output file with enriched terms: GO_output_enrichment.xlsx
- output file listing GO terms each protein in the analysis: GO_output_tems.xlsx